Recent results on hot and dense matter from the lattice

CLAUDIA RATTI

UNIVERSITY OF HOUSTON

Motivating science goals

- Is there a critical point in the QCD phase diagram?
- What are the degrees of freedom in the vicinity of the phase transition?
- Where is the transition line at high density?
- What are the phases of QCD at high density?
- Are we creating a thermal medium in experiments?

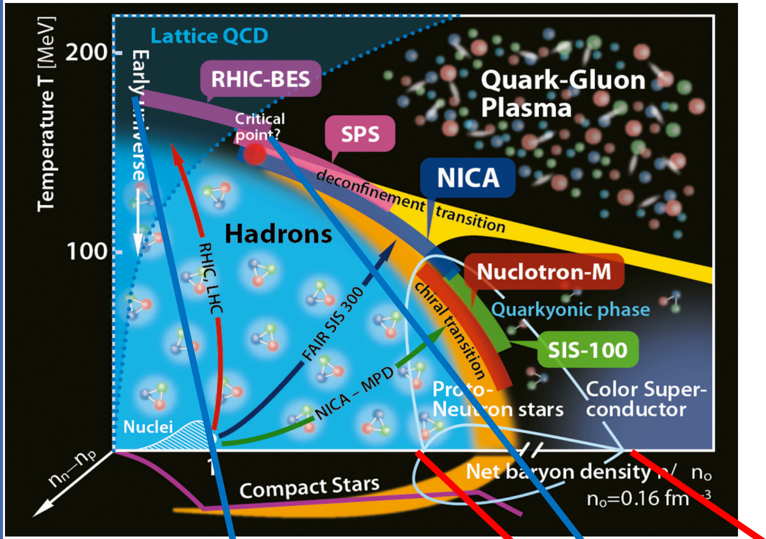

- Run 2019:
  - Collider: $\sqrt{s_{NN}}$=14.6, 19.6, 200 GeV
  - Fixed target: $\sqrt{s_{NN}}$=3.2 GeV
- Run 2020:
  - Collider: $\sqrt{s_{NN}}$=9.2, 11.5 GeV
  - Fixed target: $\sqrt{s_{NN}}$=3.5, 3.9, 4.5, 5.2, 6.2, 7.2, 7.7 GeV
- Run 2021:
  - Collider: $\sqrt{s_{NN}}$=7.7 GeV

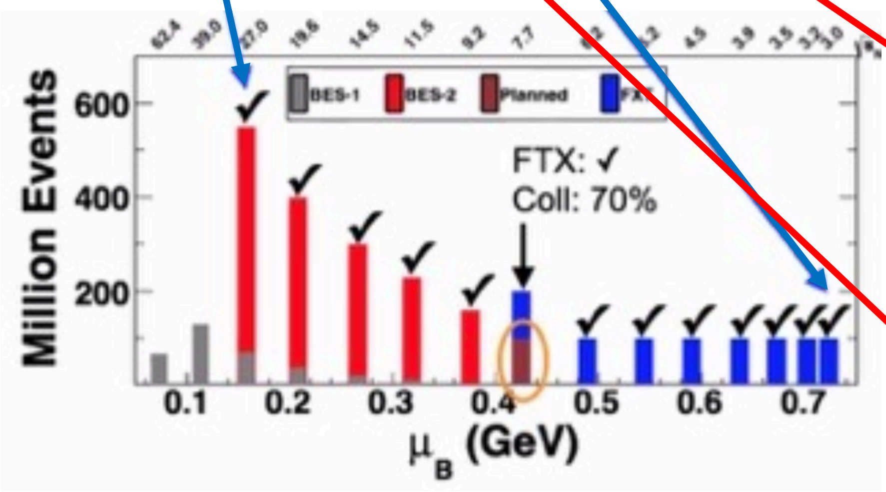

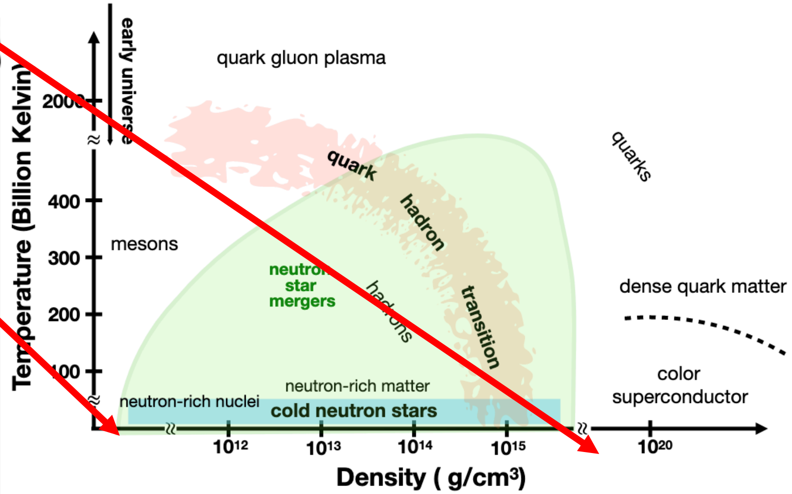

GW170817

Demonstrated the ability of mergers to advance Nuclear Physics

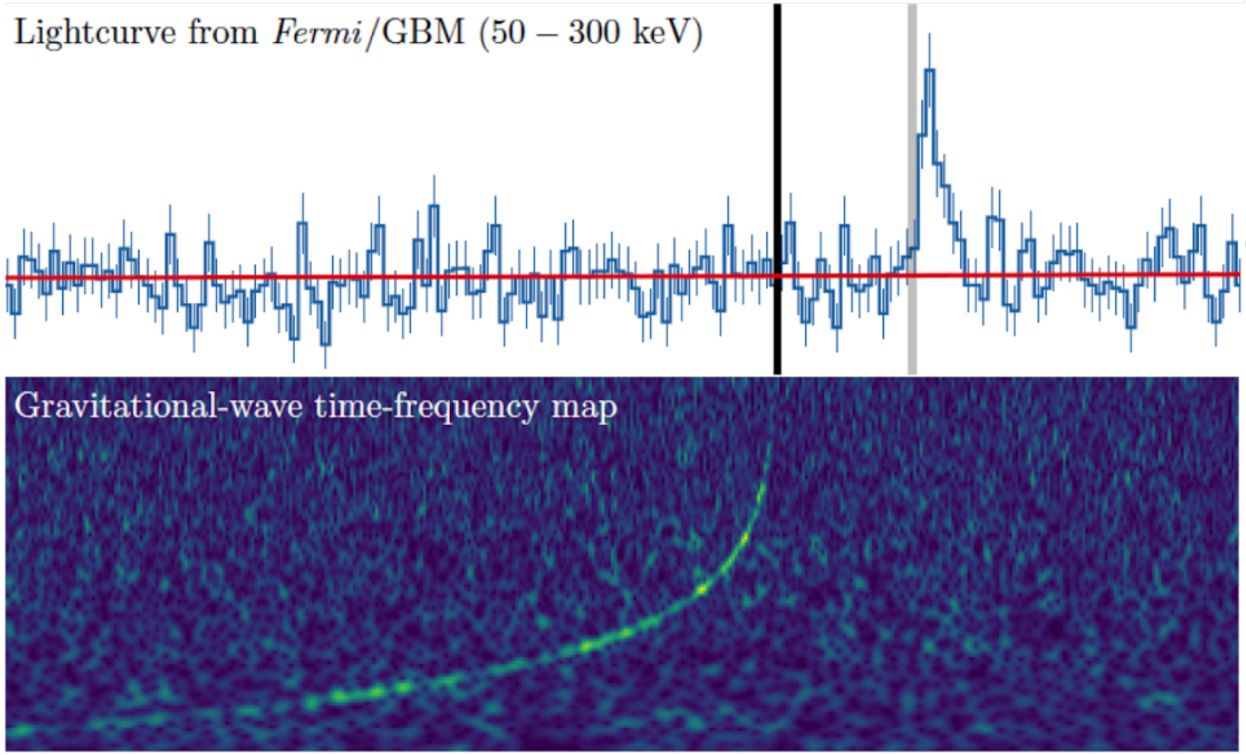

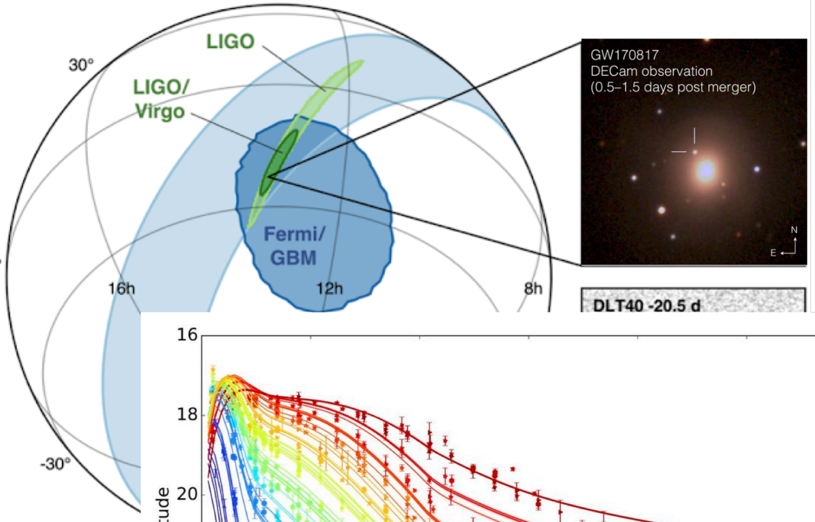

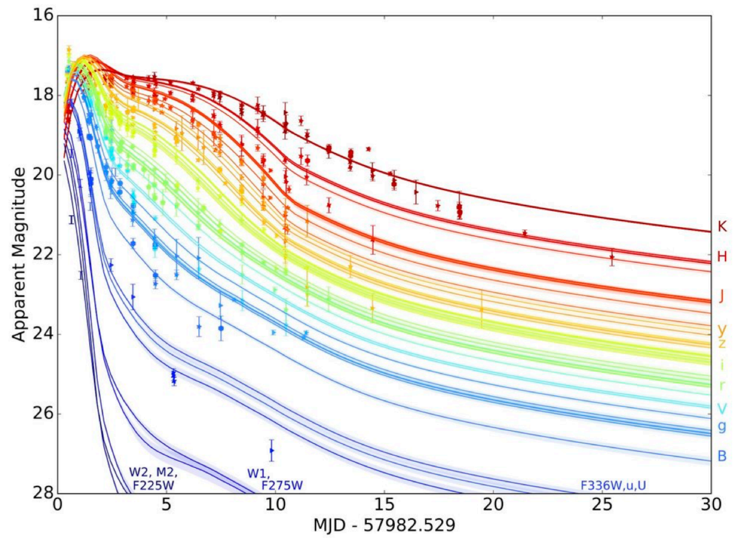

LIGO/Virgo PRL (2017)

P.S. Cowperthwaite et al., Astrophys. J. Lett. (2017)

Comparison of the facilities

Compilation by D. Cebra

CP=Critical Point

OD= Onset of Deconfinement

DHM=Dense Hadronic Matter

Facilty	RHIC BESII	SPS	NICA	SIS-100 SIS-300	J-PARC HI
Exp.:	STAR +FXT	NA61	MPD + BM@N	CBM	JHITS
Start:	2019-2021	2009	2023	2022	2025
Energy: $\sqrt{s_{NN}}$ (GeV)	7.7– 19.6 2.5-7.7	4.9-17.3	2.7 - 11 2.0-3.5	2.7-8.2	2.0-6.2
Rate: At 8 GeV	100 HZ 2000 Hz	100 HZ	<10 kHz	<10 MHZ	100 MHZ
Physics:	CP&OD	CP&OD	OD&DHM	OD&DHM	OD&DHM
	Collider Fixed target	Fixed target Lighter ion collisions	Collider Fixed target	Fixed target	Fixed target

How can lattice QCD support the experiments?

- Equation of state
  - Needed for hydrodynamic description of the QGP
- QCD phase diagram
  - Transition line at finite density
  - Constraints on the location of the critical point
- Fluctuations of conserved charges
  - Can be simulated on the lattice and measured in experiments
  - Can give information on the evolution of heavy-ion collisions
  - Can give information on the critical point

QCD transition line

$$\frac{T_c(\mu_B)}{T_c(\mu_B=0)} = 1 - \kappa_2 \left(\frac{\mu_B}{T_c(\mu_B)}\right)^2 - \kappa_4 \left(\frac{\mu_B}{T_c(\mu_B)}\right)^4$$

Observables

- We consider the following observables:

$$\langle\bar{\psi}\psi\rangle = -\left[\langle\bar{\psi}\psi\rangle_T - \langle\bar{\psi}\psi\rangle_0\right]\frac{m_{\rm ud}}{f_\pi^4}\,,$$

$$\chi = \left[\chi_T - \chi_0\right]\frac{m_{\rm ud}^2}{f_\pi^4}\,, \quad \text{with}$$

$$\langle\bar{\psi}\psi\rangle_{T,0} = \frac{T}{V}\frac{\partial \log Z}{\partial m_{\rm ud}} \qquad \chi_{T,0} = \frac{T}{V}\frac{\partial^2 \log Z}{\partial m_{\rm ud}^2}$$

- The peak height of the susceptibility indicates the strength of the transition

- The peak position in temperature serves as a definition for the chiral cross-over temperature

Observables

- Plan:
  - Calculate these two observables at finite imaginary μ_B and finite temperature T
  - Use the shift of these observables as a function of imaginary μ_B to determine T_c, κ_2 and κ_4

S. Borsanyi et al., PRL 2020

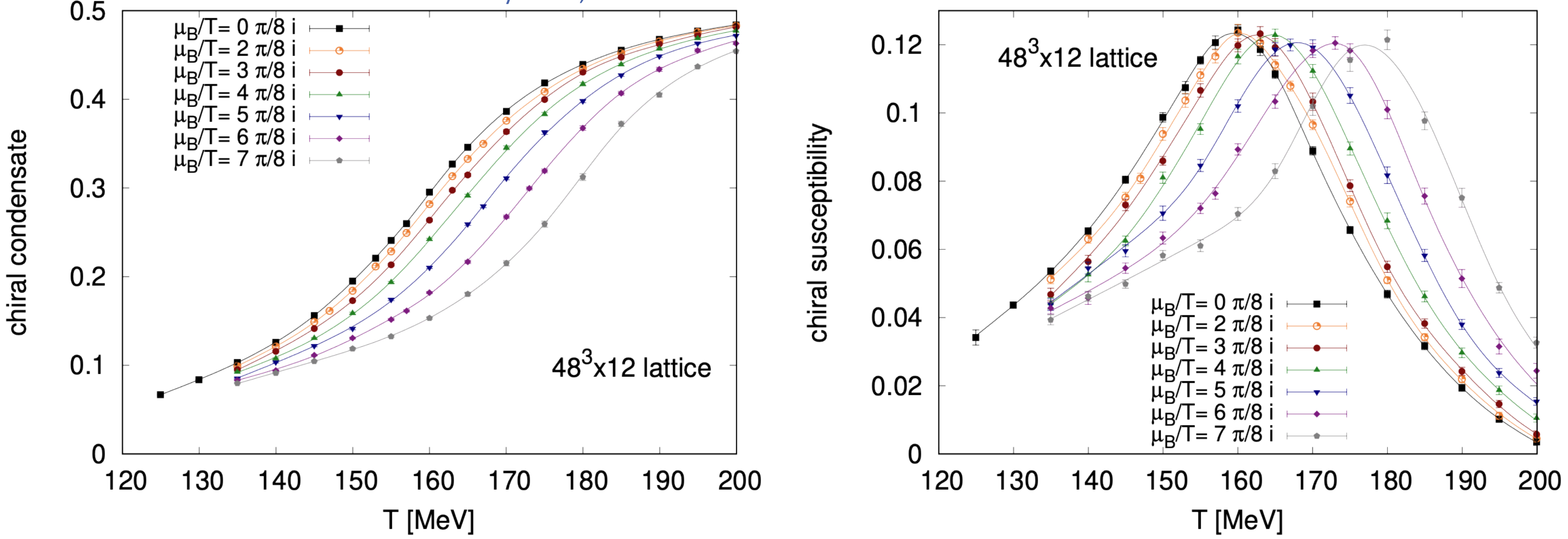

Observables

- Observation
  - When we plot the chiral susceptibility as a function of the chiral condensate, we observe a very weak chemical potential dependence

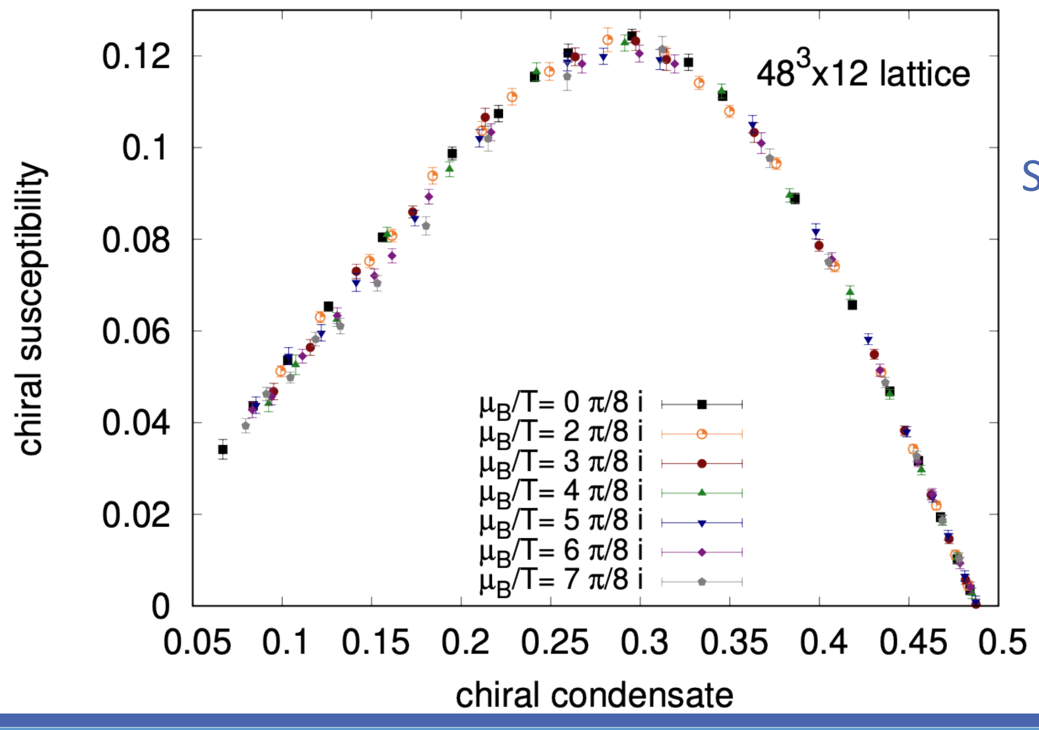

S. Borsanyi et al., PRL 2020

Procedure

- Find the peak in the curve $\chi(\langle\bar{\psi}\psi\rangle)$ through a low-order polynomial fit for each N_t and imaginary μ_B. This yields $\langle\bar{\psi}\psi\rangle_c$
- Use an interpolation of $\langle\bar{\psi}\psi\rangle(T)$ to convert $\langle\bar{\psi}\psi\rangle_c$ to T_c for each N_t and imaginary μ_B.
- Perform a fit of $T_c(N_t, \mathrm{Im}\mu_B/T_c)$ to determine the coefficients K_2 and K_4
- This leads to 2^8=256 independent analyses

Results

$$T_c(LT=4,\mu_B=0) = 158.0 \pm 0.6 \text{ MeV}$$
$$\kappa_2 = 0.0153 \pm 0.0018 \,,$$
$$\kappa_4 = 0.00032 \pm 0.00067$$

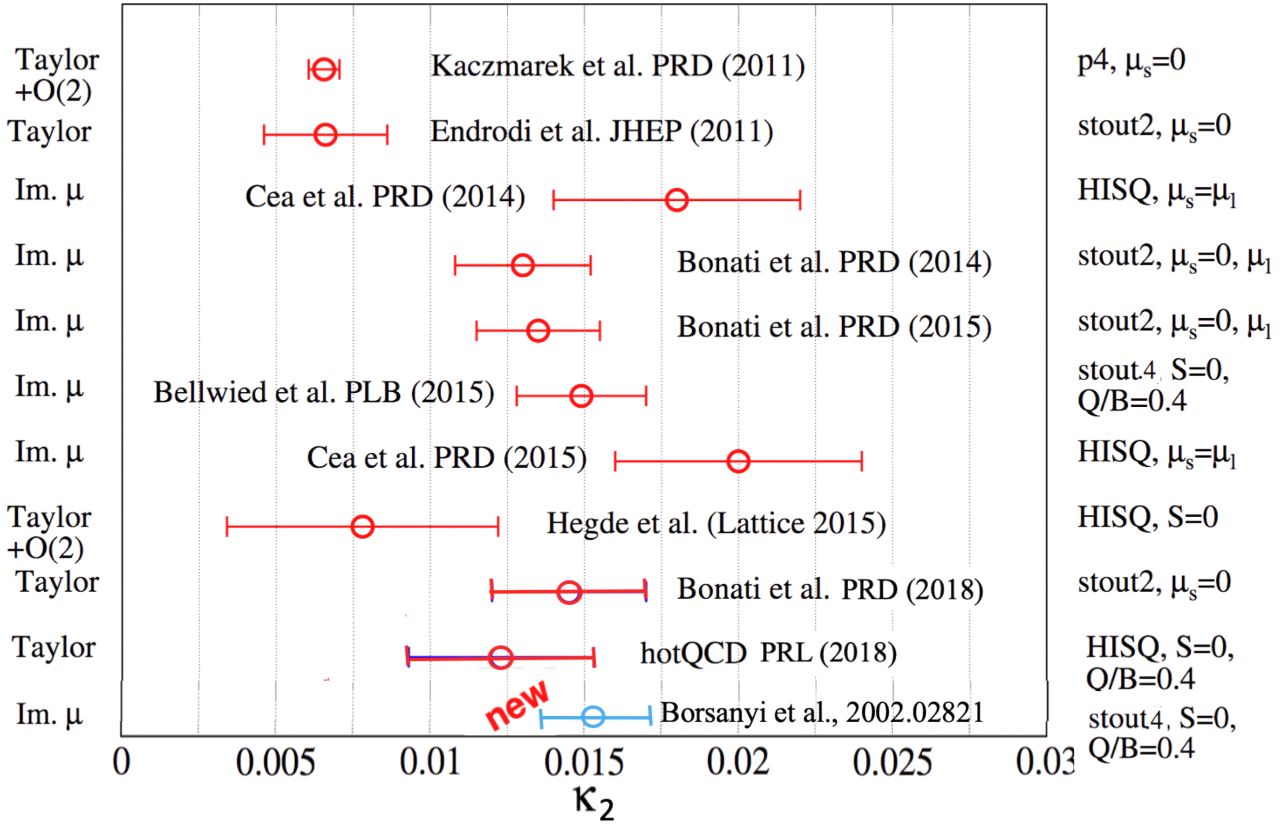

Results

$$T_c(LT = 4, \mu_B = 0) = 158.0 \pm 0.6 \text{ MeV}$$
$$\kappa_2 = 0.0153 \pm 0.0018 ,$$
$$\kappa_4 = 0.00032 \pm 0.00067$$

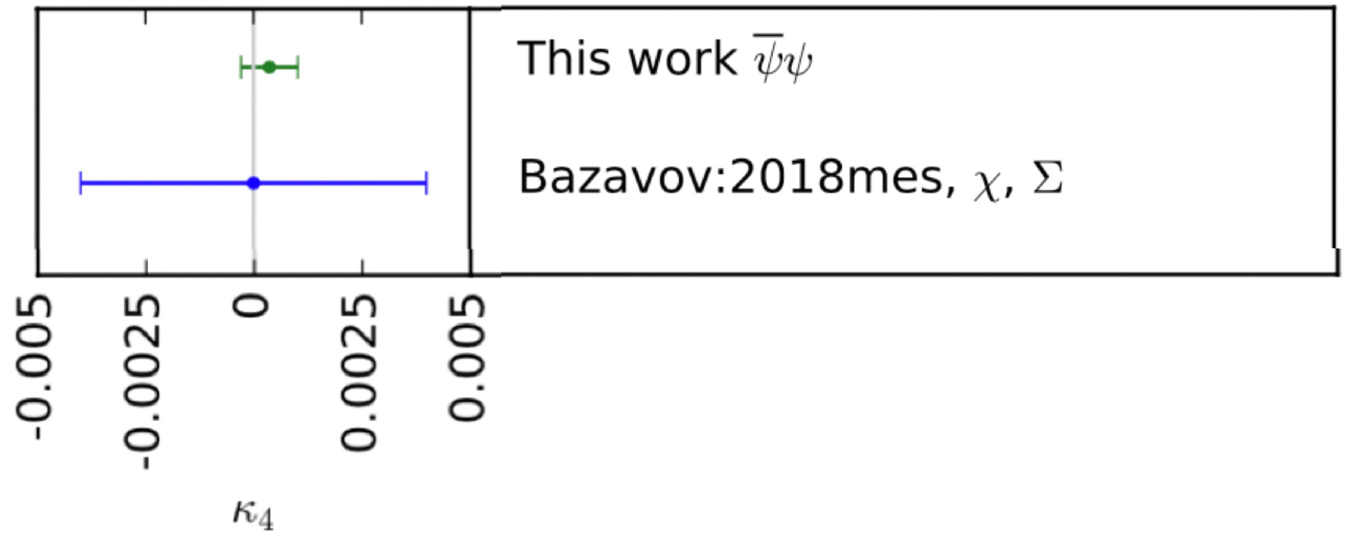

Width of the transition

S. Borsanyi et al., PRL 2020

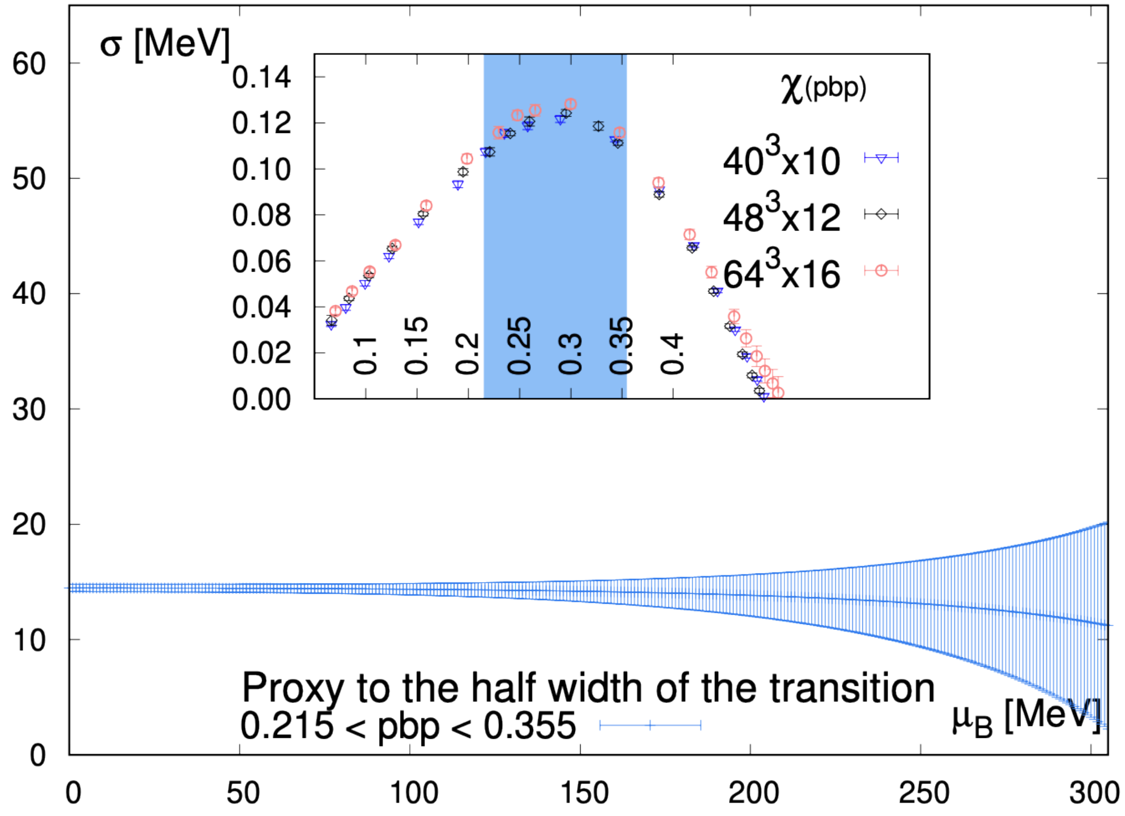

- The width of the transition is constant up to μ_B~300 MeV

Strength of the transition

- Height of the peak of the chiral susceptibility at the crossover temperature: proxy for the strength of the crossover

S. Borsanyi et al., PRL 2020

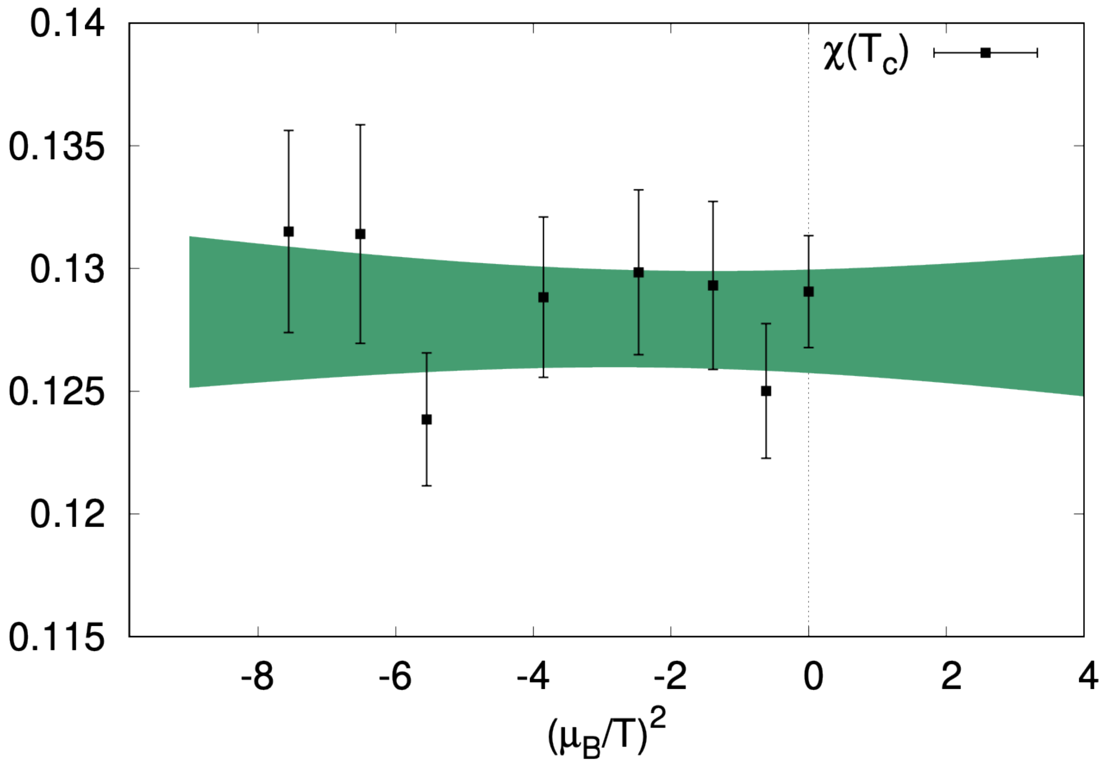

QCD Equation of State at finite density

TAYLOR EXPANSION

NEW EXPANSION SCHEME

QCD EoS at μ_B=0

WB: PLB (2014); HotQCD: PRD (2014)

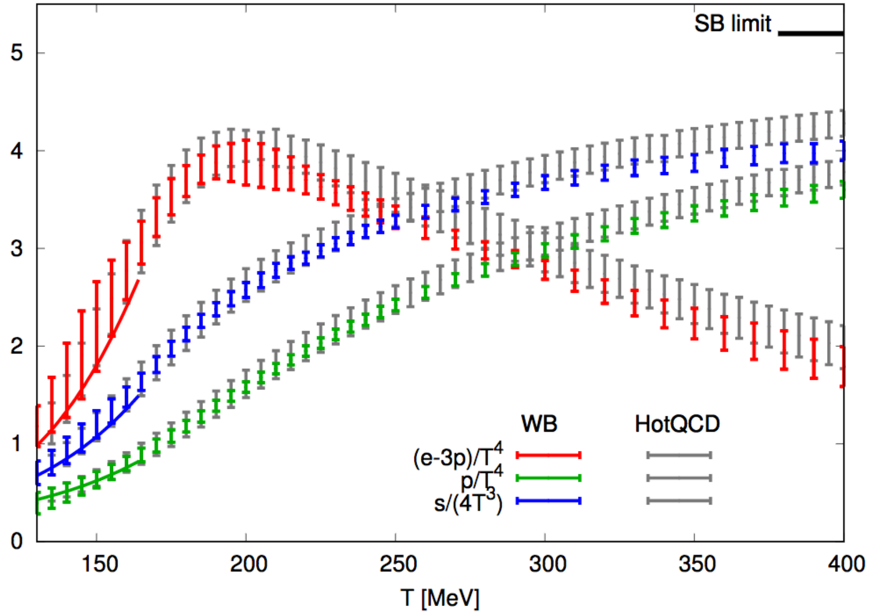

WB: Nature (2016)

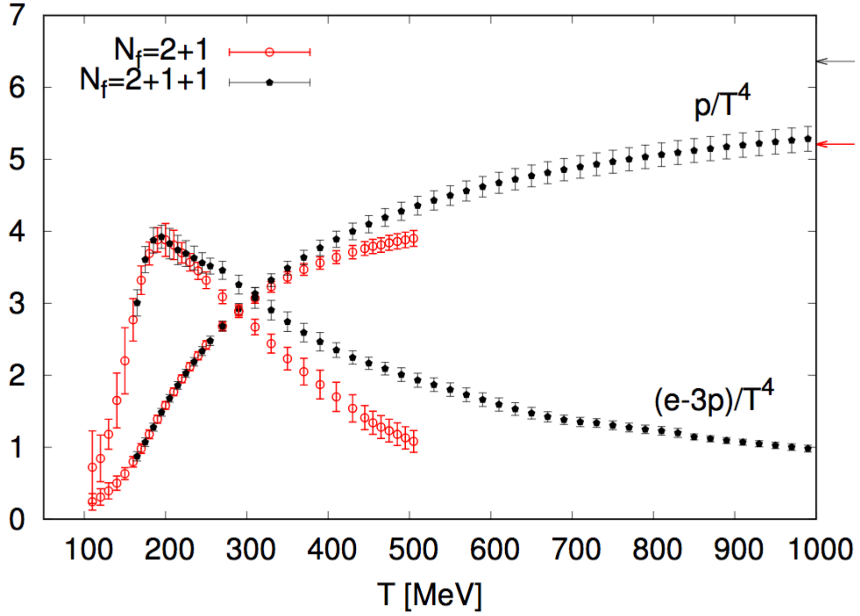

- EoS for N_f=2+1 known in the continuum limit since 2013
- Good agreement with the HRG model at low temperature
- Charm quark relevant degree of freedom already at T~250 MeV

Constraints on the EoS from the experiments

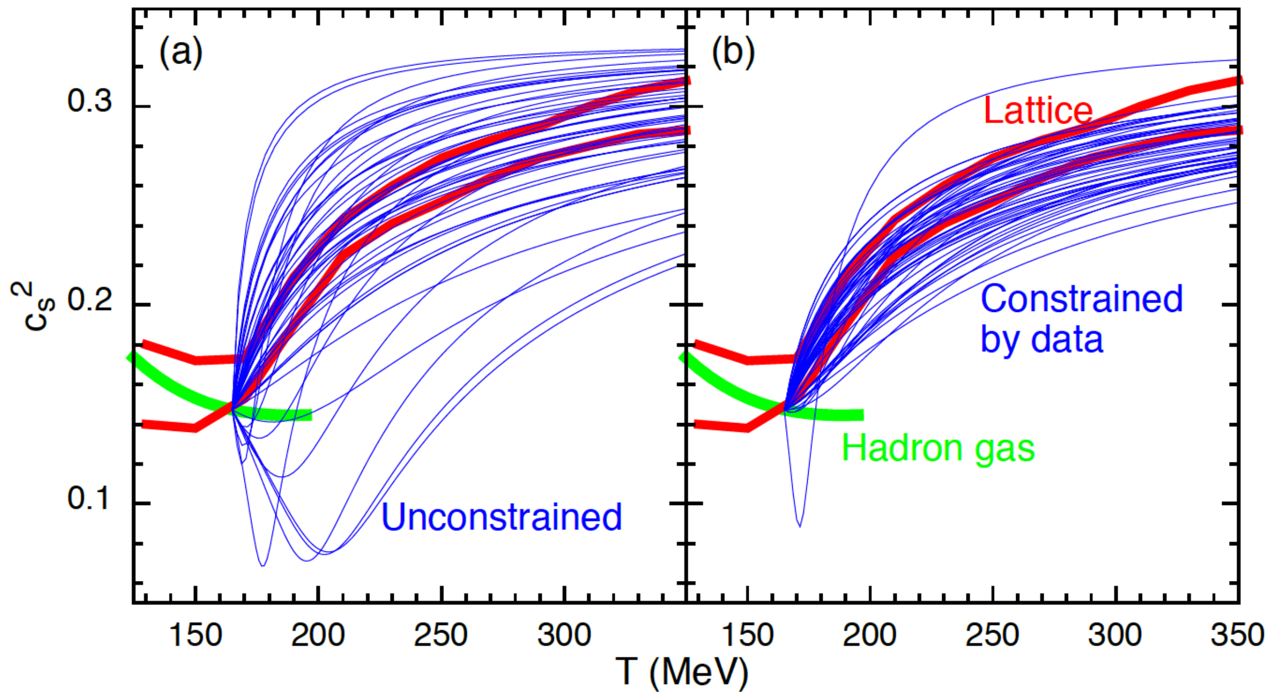

S. Pratt et al., PRL (2015)

- Comparison of data from RHIC and LHC to theoretical models through Bayesian analysis
- The posterior distribution of EoS is consistent with the lattice QCD one

Fermionic sign problem

- The QCD path integral is computed by Monte Carlo algorithms which sample field configurations with a weight proportional to the exponential of the action

$$Z(\mu_B, T) = \mathrm{Tr}\left(e^{-\frac{H_{QCD}-\mu_B N_B}{T}}\right) = \int \mathcal{D}U e^{-S_G[U]} \det M[U, \mu_B]$$

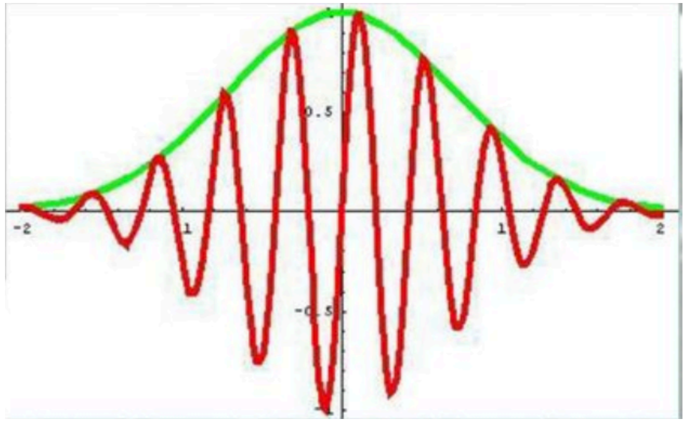

- $\det M[\mu_B]$ complex → Monte Carlo simulations are not feasible
- We can rely on a few approximate methods, viable for small μ_B/T:
  - Taylor expansion of physical quantities around $\mu_B=0$

    Bielefeld-Swansea collaboration 2002; R. Gavai, S. Gupta 2003
  - Simulations at imaginary chemical potentials

    Alford, Kapustin, Wilczek, 1999; de Forcrand, Philipsen, 2002; D'Elia, Lombardo 2003

Taylor expansion of EoS

- Taylor expansion of the pressure:

χ_{2n}^{B}

$$\frac{p(T,\mu_B)}{T^4} = \frac{p(T,0)}{T^4} + \sum_{n=1}^{\infty} \frac{1}{(2n)!} \left. \frac{\mathrm{d}^{2n}(p/T^4)}{d(\frac{\mu_B}{T})^{2n}} \right|_{\mu_B=0} \left(\frac{\mu_B}{T}\right)^{2n} = \sum_{n=0}^{\infty} c_{2n}(T) \left(\frac{\mu_B}{T}\right)^{2n}$$

<u>Simulations at imaginary μ_B</u>:

Continuum, O(10^4) configurations, errors include systematics

WB: NPA (2017)

c_2

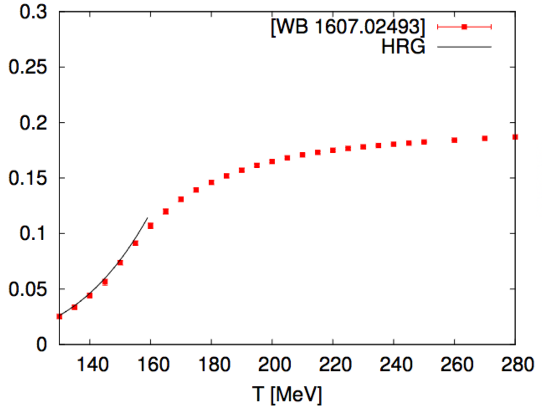

c_4

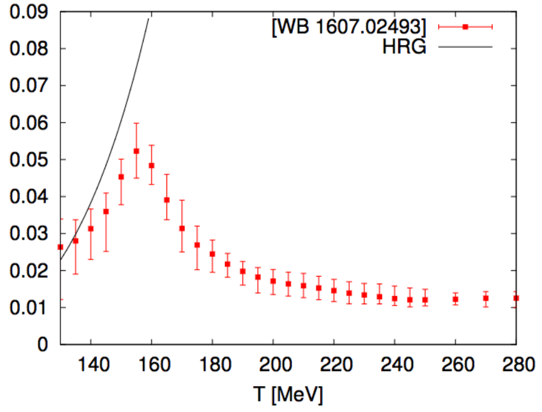

c_6

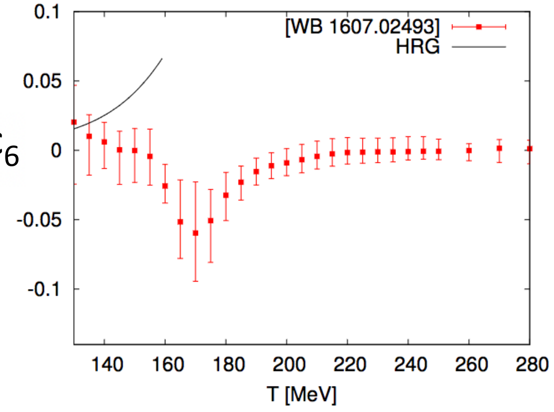

See also: HotQCD, PRD (2017), PRD (2022)

Taylor expansion of EoS

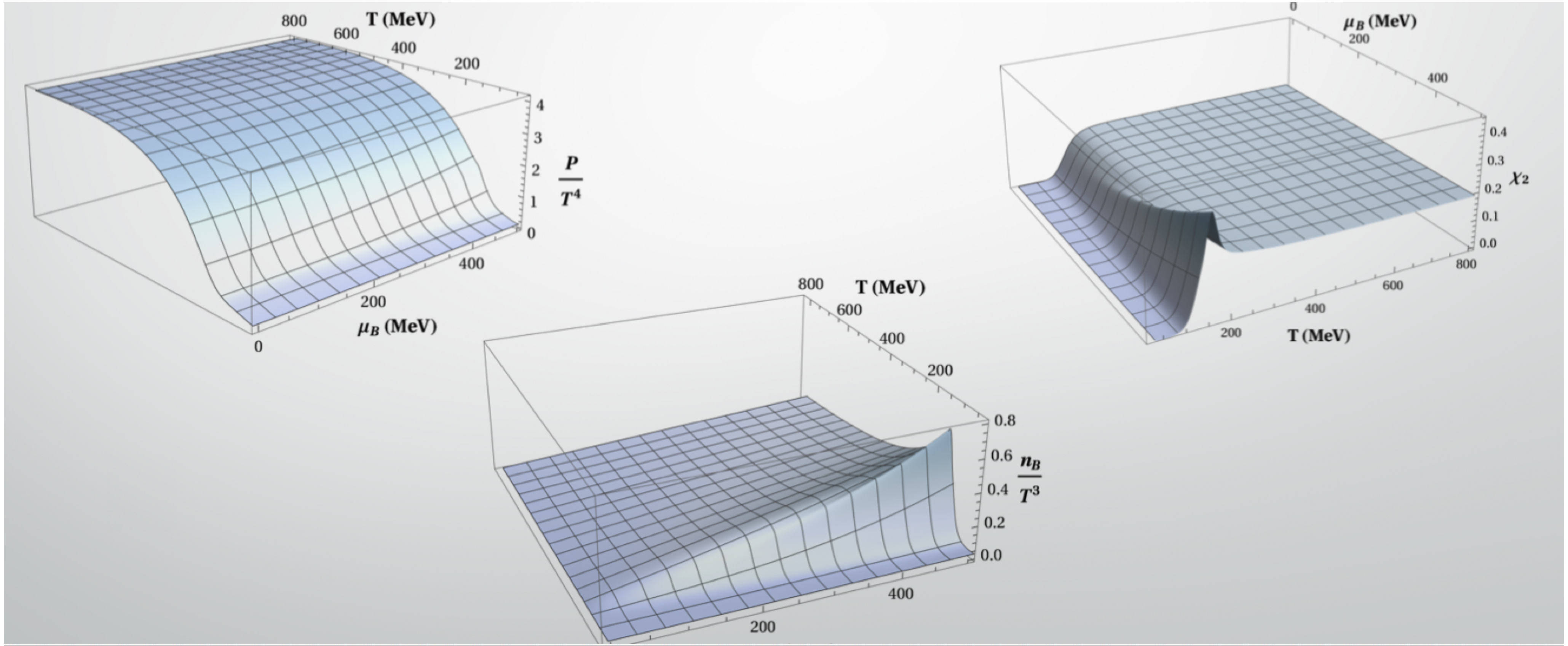

Range of validity of equation of state

- We now have the equation of state for $\mu_B/T \leq 2$ or in terms of the RHIC energy scan:

$$\sqrt{s} = 200,\ 62.4,\ 39,\ 27,\ 19.6,\ 14.5\text{GeV}$$

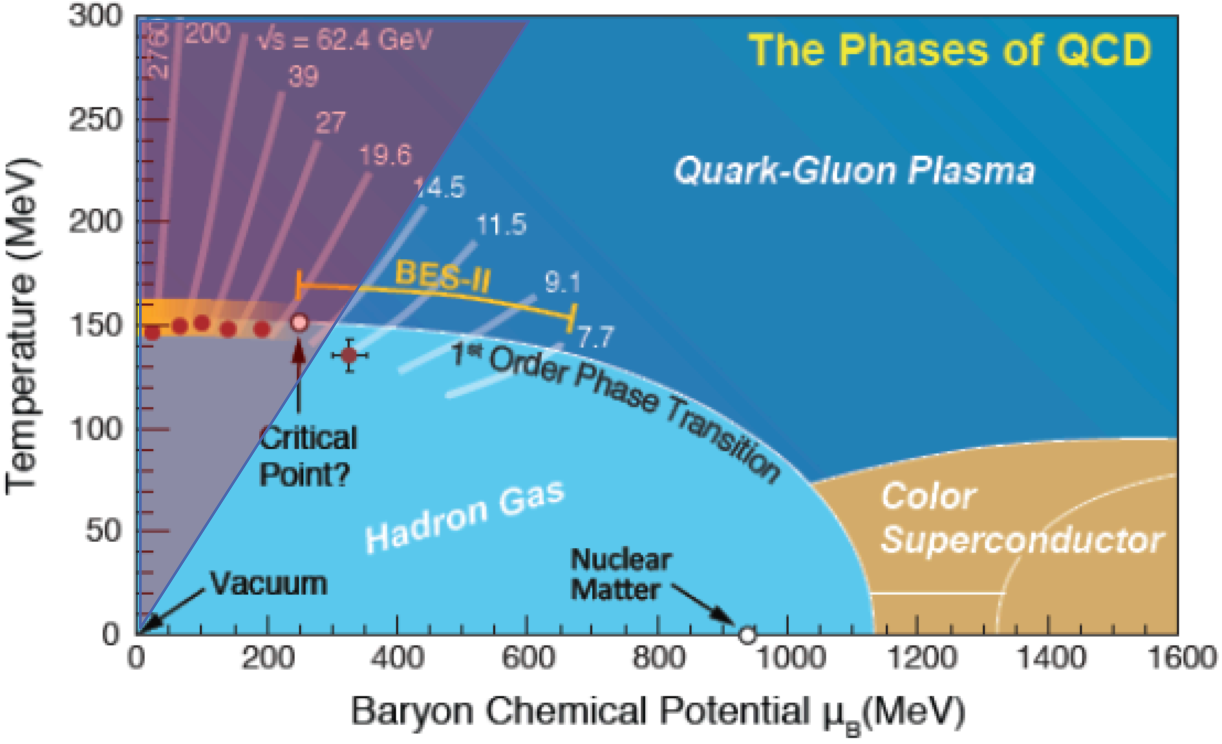

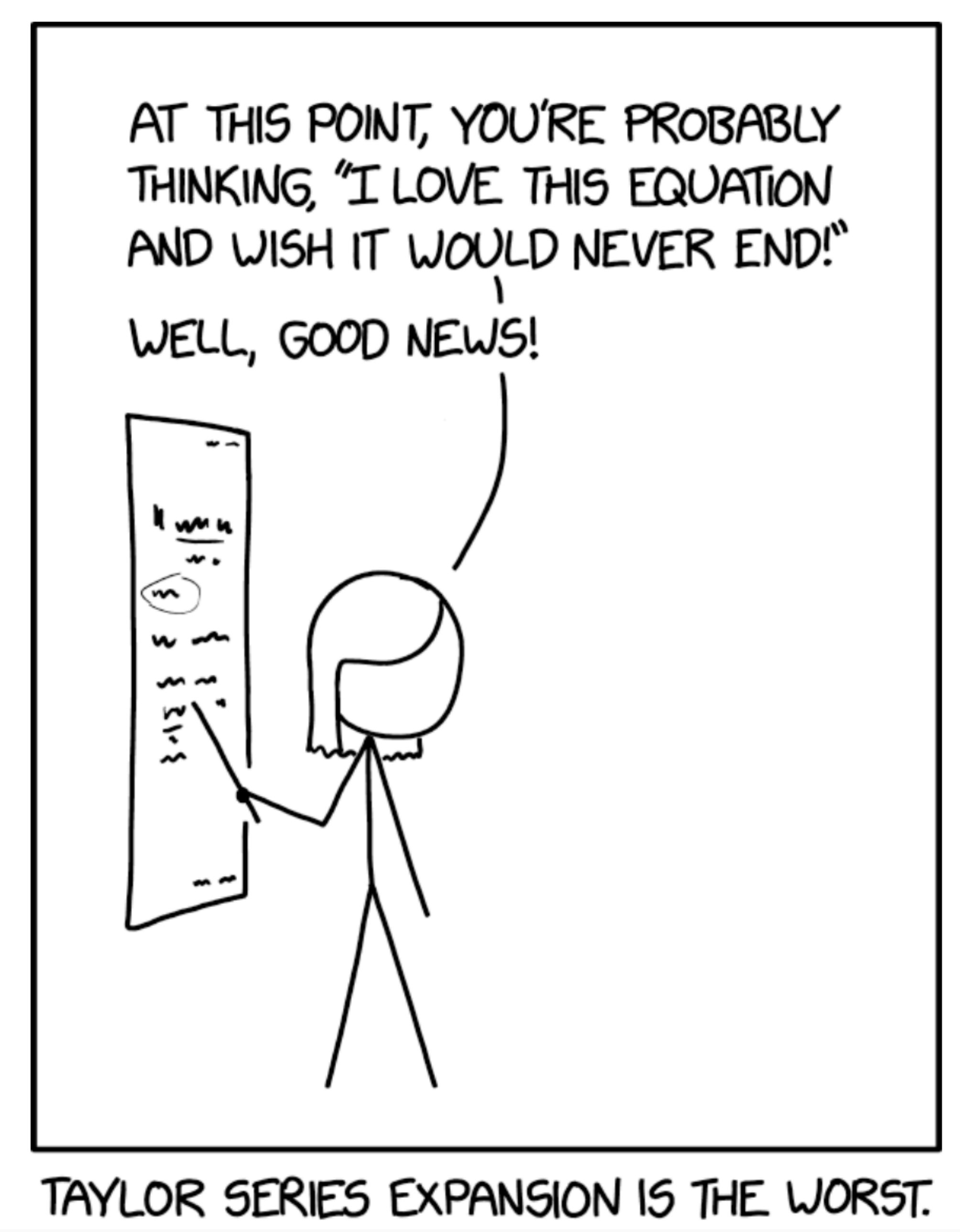
AT THIS POINT, YOU'RE PROBABLY THINKING, "I LOVE THIS EQUATION AND WISH IT WOULD NEVER END!"
WELL, GOOD NEWS!
TAYLOR SERIES EXPANSION IS THE WORST.

Problems with Taylor series

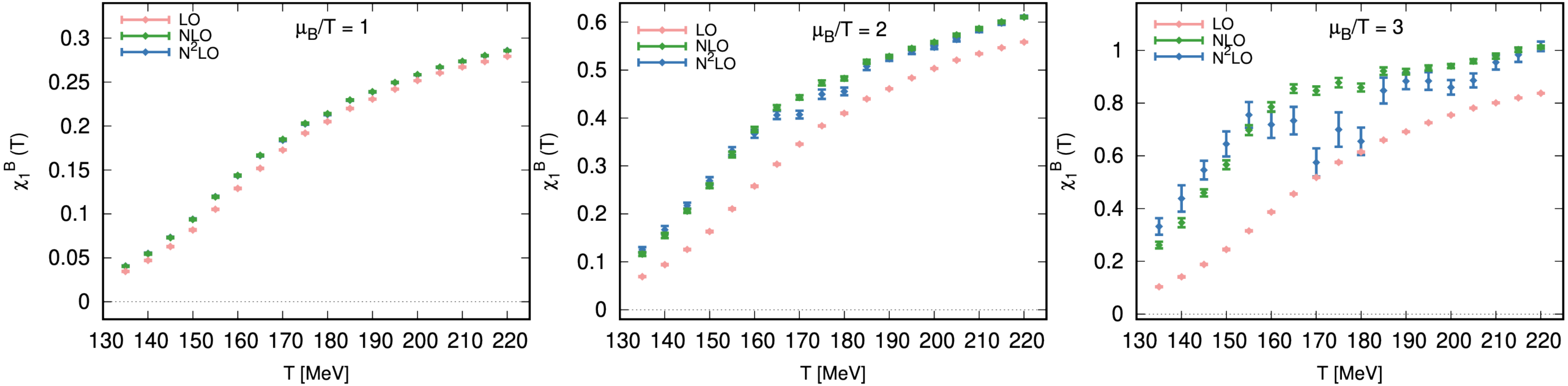

- ❑ Poor convergence of Taylor series: need to sum many terms to reach high μ_B
- ❑ Oscillatory/non-monotonic behavior in some observables at high μ_B
  - ➢ Unphysical, due to truncation of Taylor series

An alternative approach

From simulations at imaginary μ_B we *observe* that $\chi_1^B(T, \hat{\mu}_B)$ at (imaginary) $\hat{\mu}_B$ appears to be differing from $\chi_2^B(T, 0)$ mostly by a rescaling of T:

$$\frac{\chi_1^B(T, \hat{\mu}_B)}{\hat{\mu}_B} = \chi_2^B(T', 0) \ , \quad T' = T\left(1 + \kappa\, \hat{\mu}_B^2\right)$$

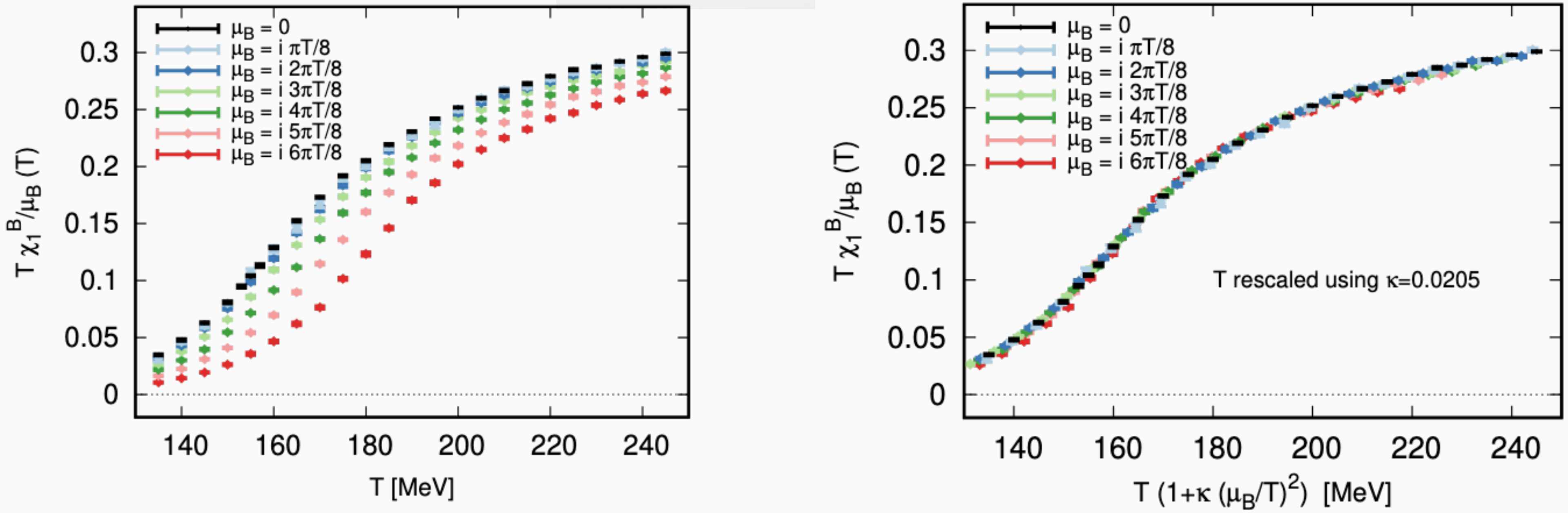

Taylor expanding a (shifting) sigmoid

Assume we have a sigmoid function $f(T)$ which shifts with $\hat{\mu}$, with a simple T-independent shifting parameter κ. How does Taylor cope with it?

$$f(T, \hat{\mu}) = f(T', 0) \ , \qquad T' = T(1 + \kappa \hat{\mu}^2) \ ,$$

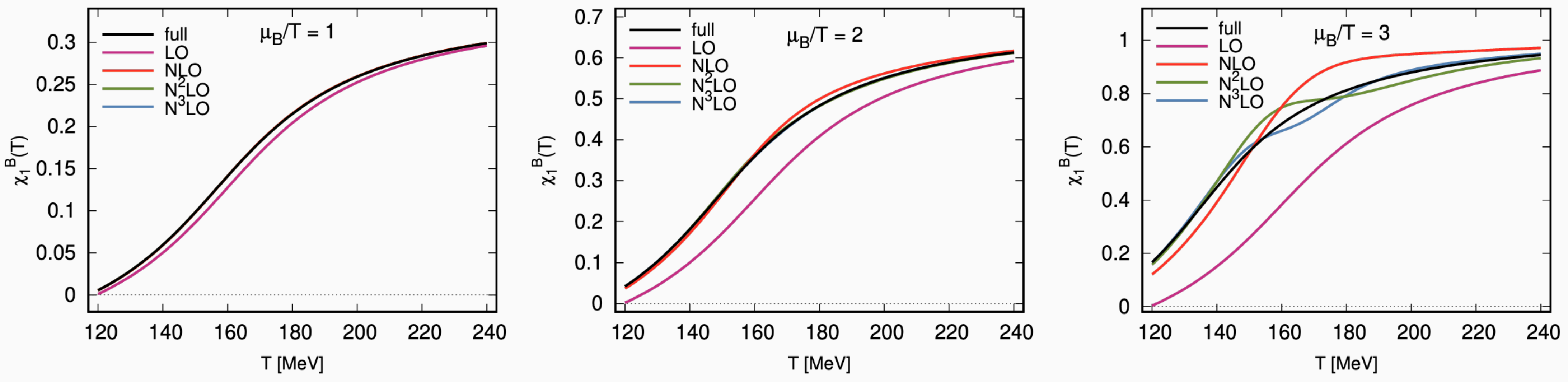

We fitted $f(T, 0) = a + b \arctan(c(T - d))$ to $\chi_2^B(T, 0)$ data for a 48×12 lattice

Taylor expanding a (shifting) sigmoid

- The Taylor expansion seems to have problems reproducing the original function (left)
- Quite suggestive comparison with actual Taylor-expanded lattice data (right)

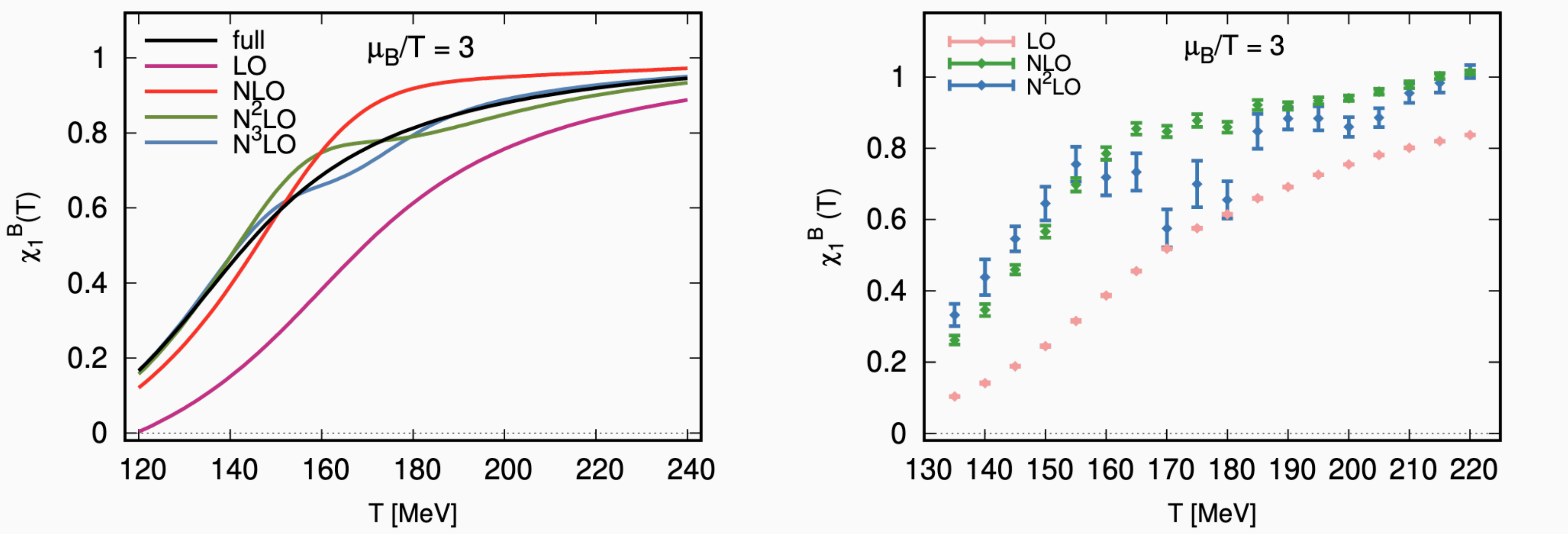

- Problems at T slightly larger than T_{pc} ⇒ influence from structure in χ_6^B and χ_8^B

Formulation

- We have observed the $\hat{\mu}_B$-dependence seems to amount to a simple T- rescaling
- A simplistic scenario with a single T- independent parameter κ does not provide a systematic treatment which can serve as an alternative expansion scheme
- We allow for more than $\mathcal{O}(\hat{\mu}^2)$ expansion of T' and let the coefficients be $T-$dependent:

$$\frac{\chi_1^B(T,\hat{\mu}_B)}{\hat{\mu}_B} = \chi_2^B(T',0)\ , \quad T' = T\left(1 + \kappa_2(T)\,\hat{\mu}_B^2 + \kappa_4(T)\,\hat{\mu}_B^4 + \mathcal{O}(\hat{\mu}_B^6)\right)$$

- **Important:** we are simply re-organizing the Taylor expansion via an expansion in the shift

$$\Delta T = T - T' = \left(\kappa_2(T)\,\hat{\mu}_B^2 + \kappa_4(T)\,\hat{\mu}_B^4 + \mathcal{O}(\hat{\mu}_B^6)\right)$$

- Comparing the (Taylor) expansion in $\hat{\mu}_B$ and our expansion in ΔT order by order, we can relate $\chi_n^B(T)$ and $\kappa_n(T)$

Formulation

Equating same-order terms, we find

$$\chi_4^B(T) = 6T\kappa_2^{BB}(T)\frac{d\chi_2}{dT} \ ,$$

$$\chi_6^B(T) = 60T^2(\kappa_2^{BB})^2(T)\frac{d^2\chi_2}{dT^2} + 120T\kappa_4^{BB}(T)\frac{d\chi_2}{dT}$$

or, analogously:

$$\kappa_2^{BB}(T) = \frac{1}{6T}\frac{\chi_4^B(T)}{\chi_2^{B\prime}(T)} \ ,$$

$$\kappa_4^{BB}(T) = \frac{1}{360\chi_2^{B\prime}(T)^3}\left(3\chi_2^{B\prime}(T)^2\chi_6^B(T) - 5\chi_2^{B\prime\prime}(T)\chi_4^B(T)^2\right)$$

Analysis

I. Directly determine $\kappa_2(T)$ at $\hat{\mu}_B = 0$ from the previous relation

II. From our imaginary- $\hat{\mu}_B$ simulations ($\hat{\mu}_Q = \hat{\mu}_S = 0$) we calculate:

$$\frac{T' - T}{T\,\hat{\mu}_B^2} = \kappa_2(T) + \kappa_4(T)\,\hat{\mu}_B^2 + \mathcal{O}(\hat{\mu}_B^4) = \Pi(T)$$

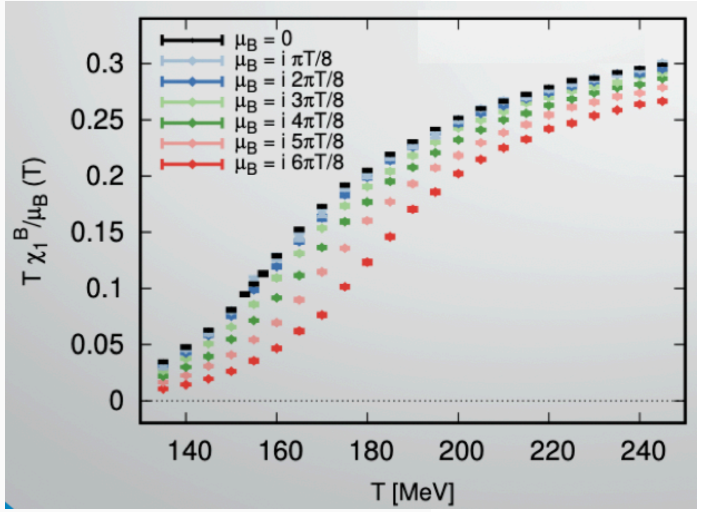

III. Calculate $\Pi(T, N_\tau, \hat{\mu}_B^2)$ for $\hat{\mu}_B = in\pi/8$ and $N_\tau = 10, 12, 16$

IV. Perform a combined fit of the $\hat{\mu}_B^2$ and $1/N_\tau^2$ dependence of $\Pi(T)$ at each temperature, yielding a continuum estimate for the coefficients

$\Rightarrow$ The $\mathcal{O}(1)$ and $\mathcal{O}(\hat{\mu}_B^2)$ coefficients of the fit are $\kappa_2(T)$ and $\kappa_4(T)$

Results for the coefficients

Our initial guess was not far-off:

- Fairly constant $\kappa_2(T)$ over a large T-range
- Clear separation in magnitude between $\kappa_2(T)$ and $\kappa_4(T)$ hints at better convergence
- Agreement with the HRG model results at low temperatures
- Polynomial fits of $\kappa_2(T)$ and $\kappa_4(T)$ before use in thermodynamics (good fit qualities)

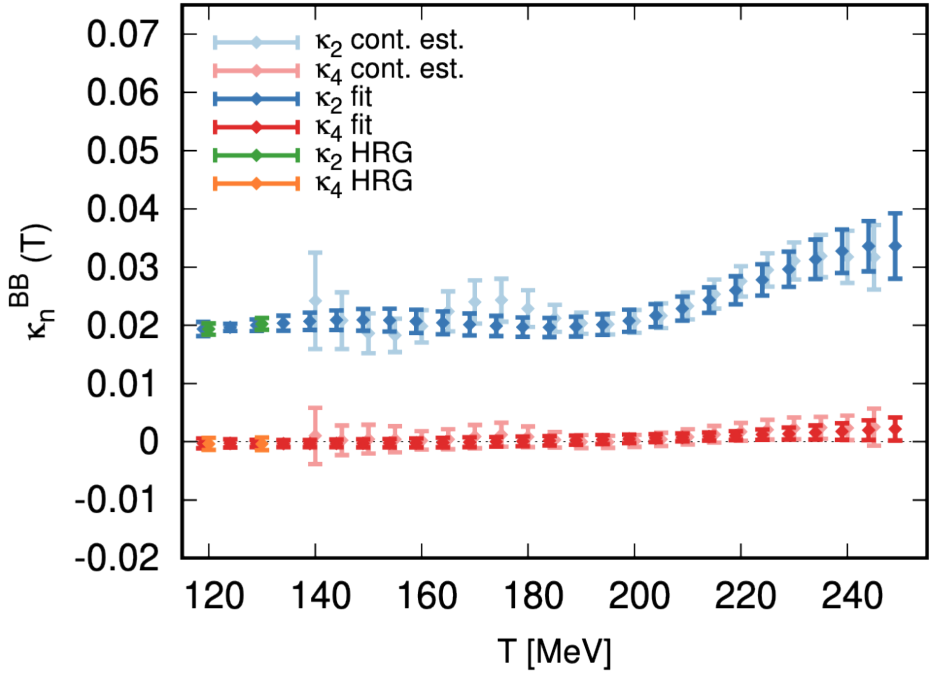

NOTE: polynomial fits take into account both statistical and systematic correlations.

Constructing the density at finite μ_B

We use the following expression:

$$\frac{\chi_1^B(T,\hat{\mu}_B)}{\hat{\mu}_B} = \chi_2^B(T',0) \ ,$$

with

$$T'(T,\hat{\mu}_B) = T\left(1 + \kappa_2^{BB}(T)\hat{\mu}_B^2 + \kappa_4^{BB}(T)\hat{\mu}_B^4 + \mathcal{O}(\hat{\mu}_B^6)\right),$$

Thermodynamics at finite μ_B

Thermodynamic quantities at finite (real) μ_B can be reconstruted from the same ansazt:

$$\frac{n_B(T,\hat{\mu}_B)}{T^3} = \hat{\mu}_B \chi_2^B(T',0)$$

with $T' = T(1 + \kappa_2^{BB}(T)\,\hat{\mu}_B^2 + \kappa_4^{BB}(T)\,\hat{\mu}_B^4)$.

From the baryon density n_B one finds the pressure:

$$\frac{p(T,\hat{\mu}_B)}{T^4} = \frac{p(T,0)}{T^4} + \int_0^{\hat{\mu}_B} \mathrm{d}\hat{\mu}'_B \frac{n_B(T,\hat{\mu}'_B)}{T^3}$$

then the entropy, energy density:

$$\frac{s(T,\hat{\mu}_B)}{T^4} = 4\frac{p(T,\hat{\mu}_B)}{T^4} + T\left.\frac{\partial p(T,\hat{\mu}_B)}{\partial T}\right|_{\hat{\mu}_B} - \hat{\mu}_B \frac{n_B(T,\hat{\mu}_B)}{T^3}$$

$$\frac{\epsilon(T,\hat{\mu}_B)}{T^4} = \frac{s(T,\hat{\mu}_B)}{T^3} - \frac{p(T,\hat{\mu}_B)}{T^4} + \hat{\mu}_B \frac{n_B(T,\hat{\mu}_B)}{T^3}$$

Thermodynamics at finite μ_B: results

- We reconstruct thermodynamic quantities up to $\hat{\mu}_B \simeq 3.5$ with uncertainties well under control
- Agreement with HRG model calculations at small temperatures
- No pathological (non-monotonic) behavior is present

S. Borsanyi, C. R. et al., PRL (2021)

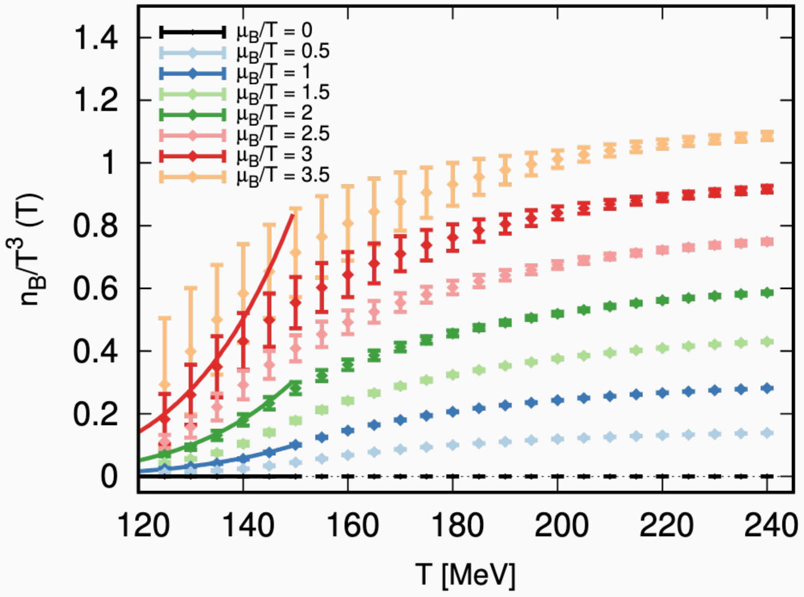

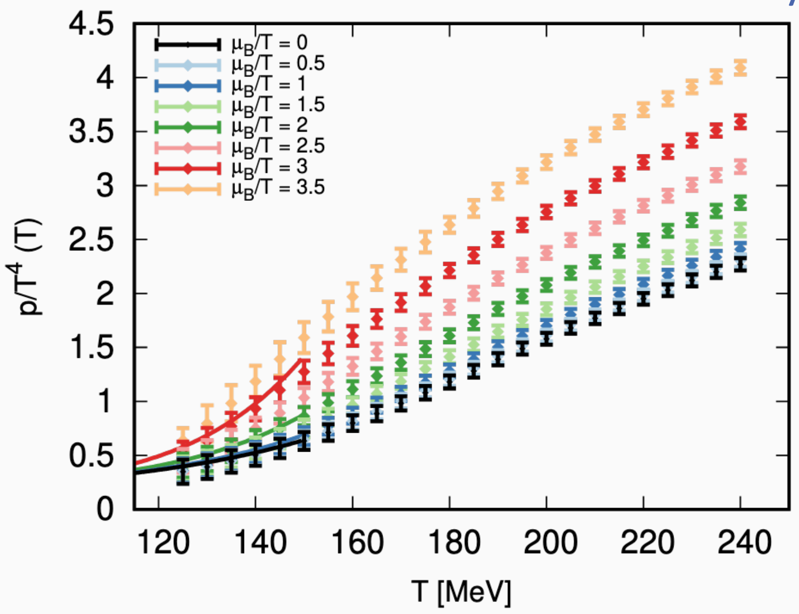

Thermodynamics at finite μ_B: results

- We reconstruct thermodynamic quantities up to $\hat{\mu}_B \simeq 3.5$ with uncertainties well under control
- Agreement with HRG model calculations at small temperatures
- No pathological (non-monotonic) behavior is present

S. Borsanyi, C. R. et al., PRL (2021)

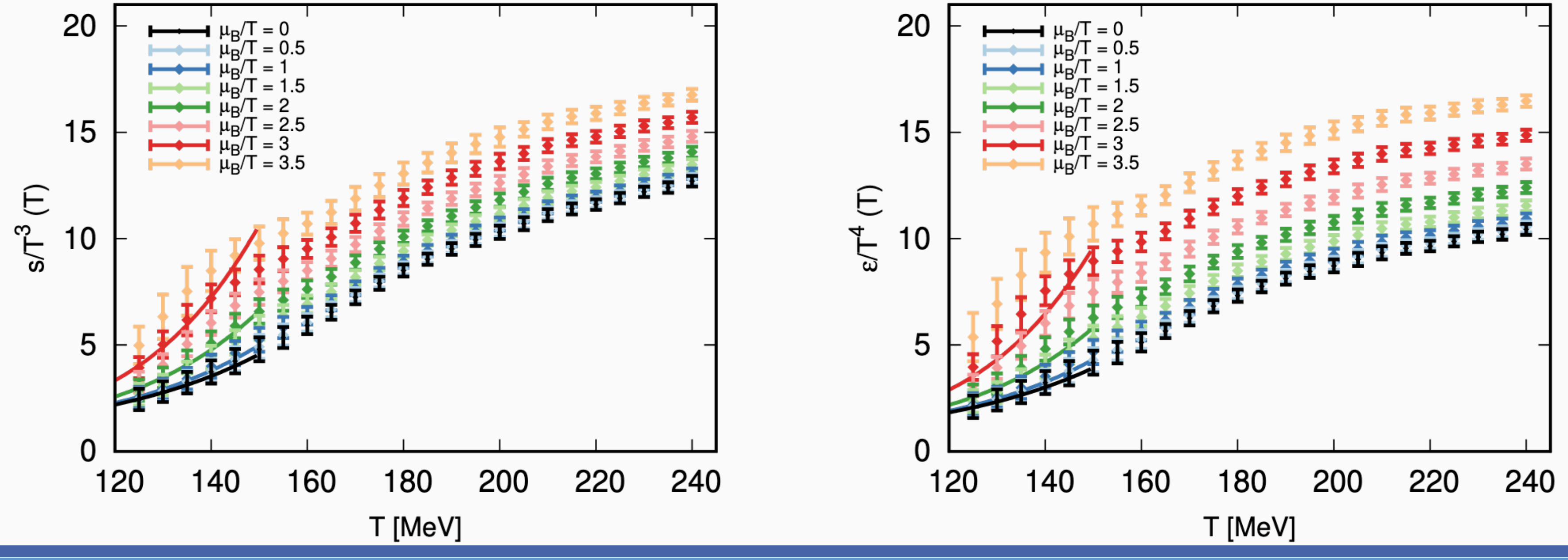

Convergence check

- We also check the results without the inclusion of $\kappa_4(T)$ (darker shades)
- Including $\kappa_4(T)$ only results in added error, but does not "move" the results

$\longrightarrow$ Good convergence

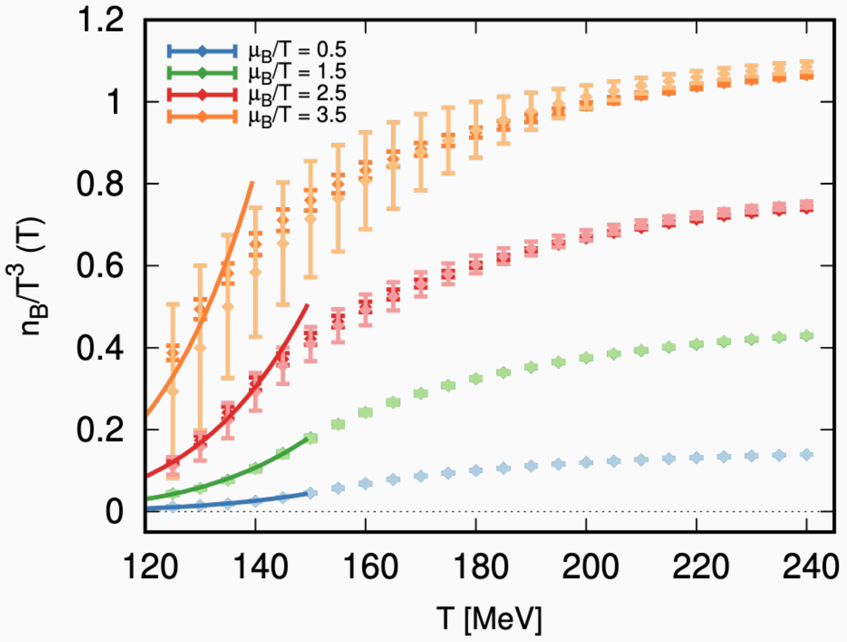

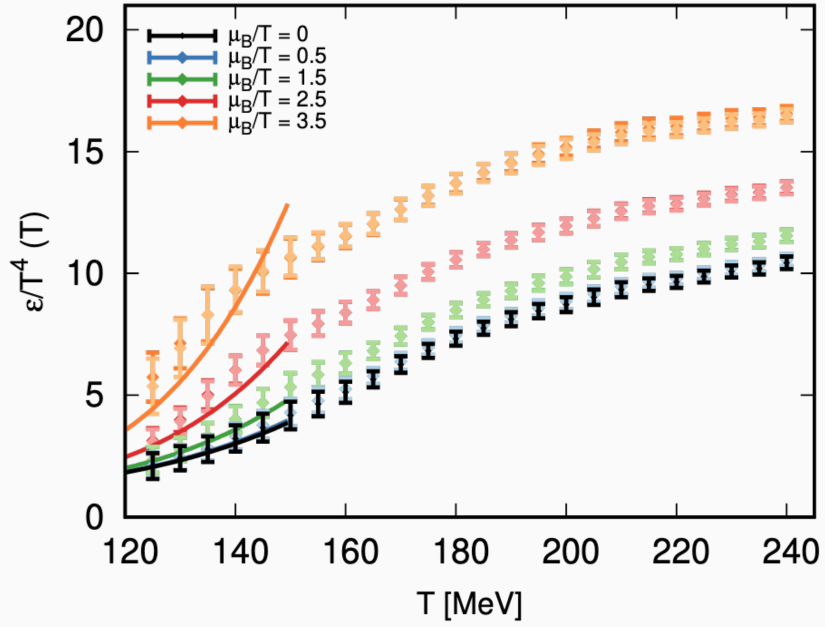

New result: strangeness-neutral EoS and beyond

- We recently extended these results to the case of strangeness-neutrality
- We expand along the strangeness-neutral line in the 4D phase diagram
- We also consider fluctuations of strangeness around the $\langle n_S \rangle=0$ condition

S. Borsanyi, C. R. et al., PRD (2022)

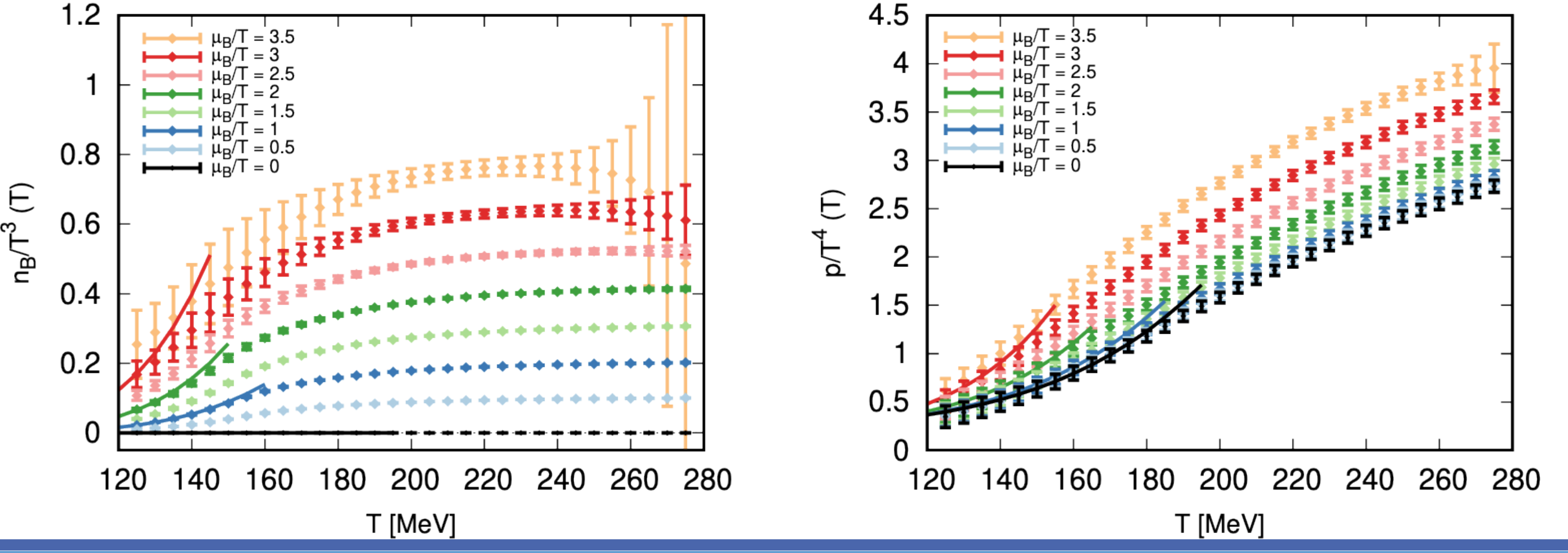

New range of validity of equation of state

- We now have the equation of state for $\mu_B/T \leq 3.5$

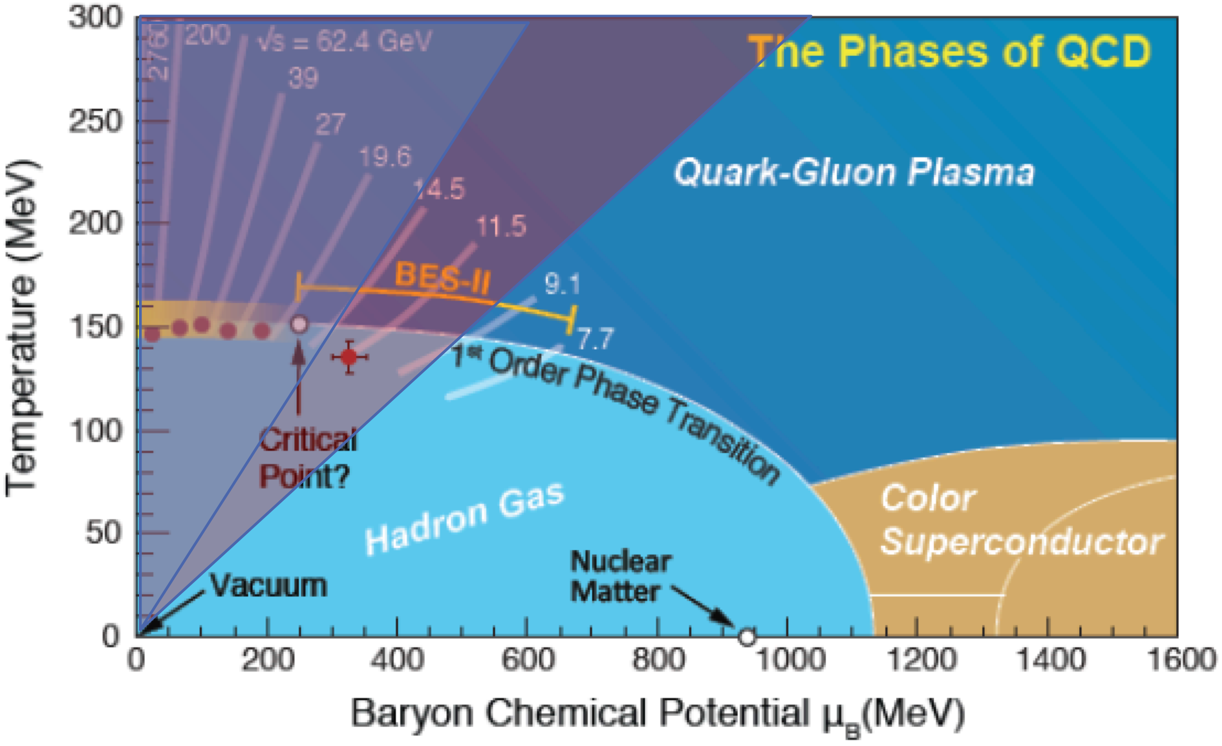

Other interesting results

- Recent development in reweighting schemes

  M. Giordano et al., JHEP 05, 088; Borsanyi et al., PRD (2022)

- Alternative ways to resum the Taylor series

  S. Mondal et al., PRL (2022); S. Mukherjee et al., PRD (2022); S. Mitra et al., 2205.08517

- Recent improvement on Taylor expansion at finite μ_B

  D. Bollweg et al., PRD (2022)

What happens at large densities?

- We need to merge the lattice QCD equation of state with other effective theories
- Careful study of their respective range of validity
- Constrain the parameters to reproduce known limits
- Test different possibilities and validate/exclude them

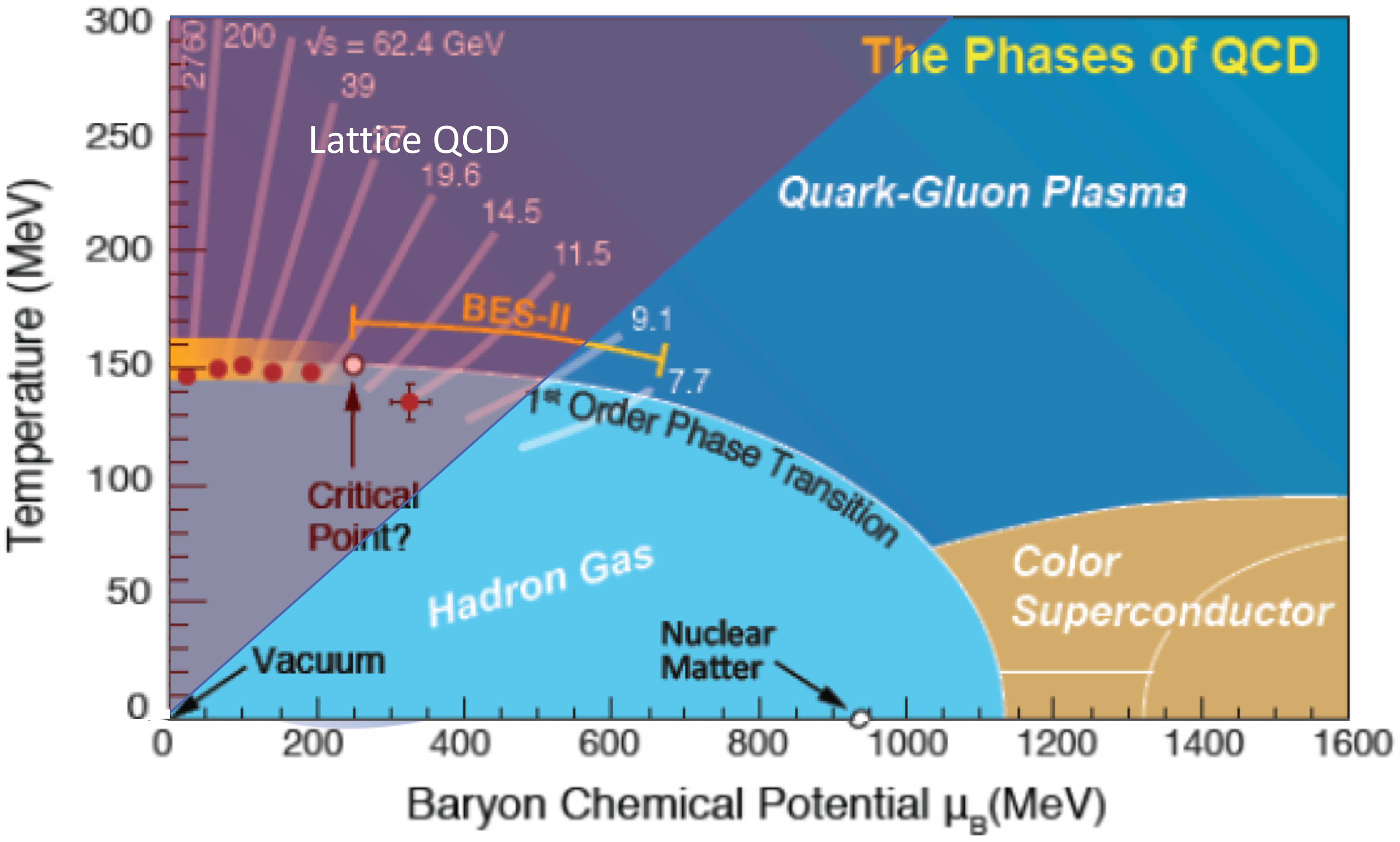

Lattice QCD: WB: PRL (2021)

What happens at large densities?

- We need to merge the lattice QCD equation of state with other effective theories
- Careful study of their respective range of validity
- Constrain the parameters to reproduce known limits
- Test different possibilities and validate/exclude them

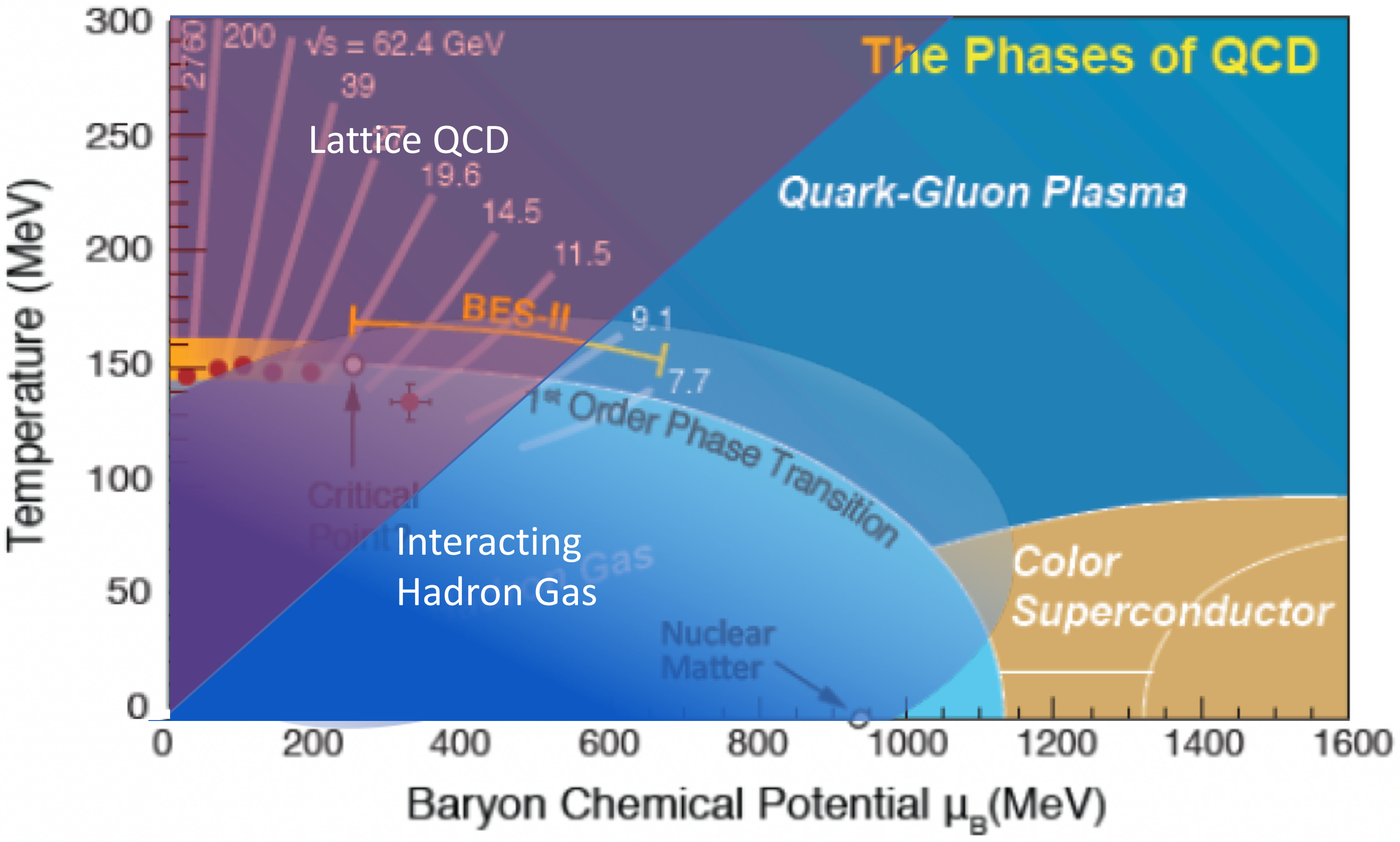

Lattice QCD: WB: PRL (2021)
Interacting HRG: V. Vovchenko et al., PRL (2017)

What happens at large densities?

- We need to merge the lattice QCD equation of state with other effective theories
- Careful study of their respective range of validity
- Constrain the parameters to reproduce known limits
- Test different possibilities and validate/exclude them

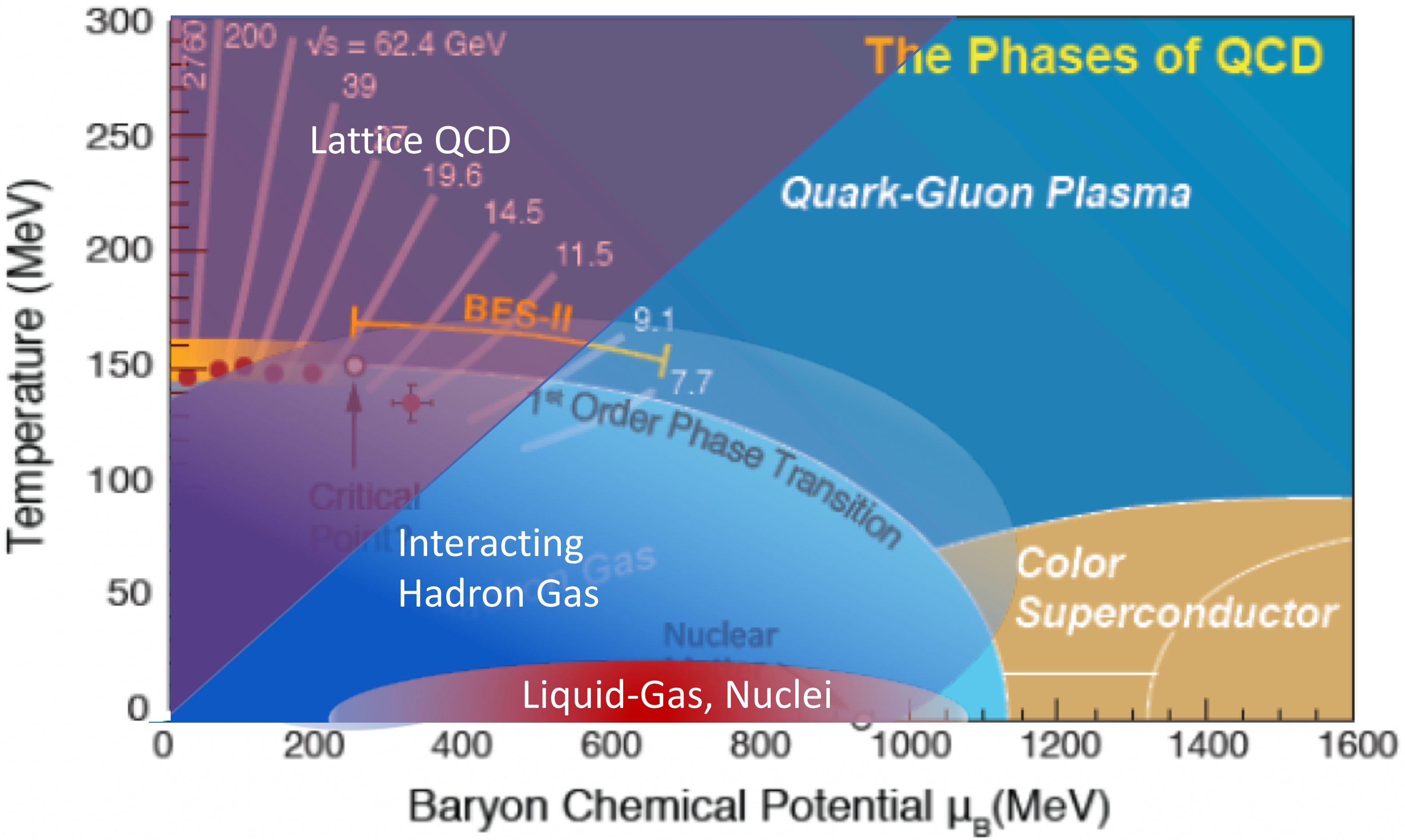

Lattice QCD: WB: PRL (2021)
Interacting HRG: V. Vovchenko et al., PRL (2017)
Liquid-gas, Nuclei: see e.g. Du et al. PRC (2019)

What happens at large densities?

- We need to merge the lattice QCD equation of state with other effective theories
- Careful study of their respective range of validity
- Constrain the parameters to reproduce known limits
- Test different possibilities and validate/exclude them

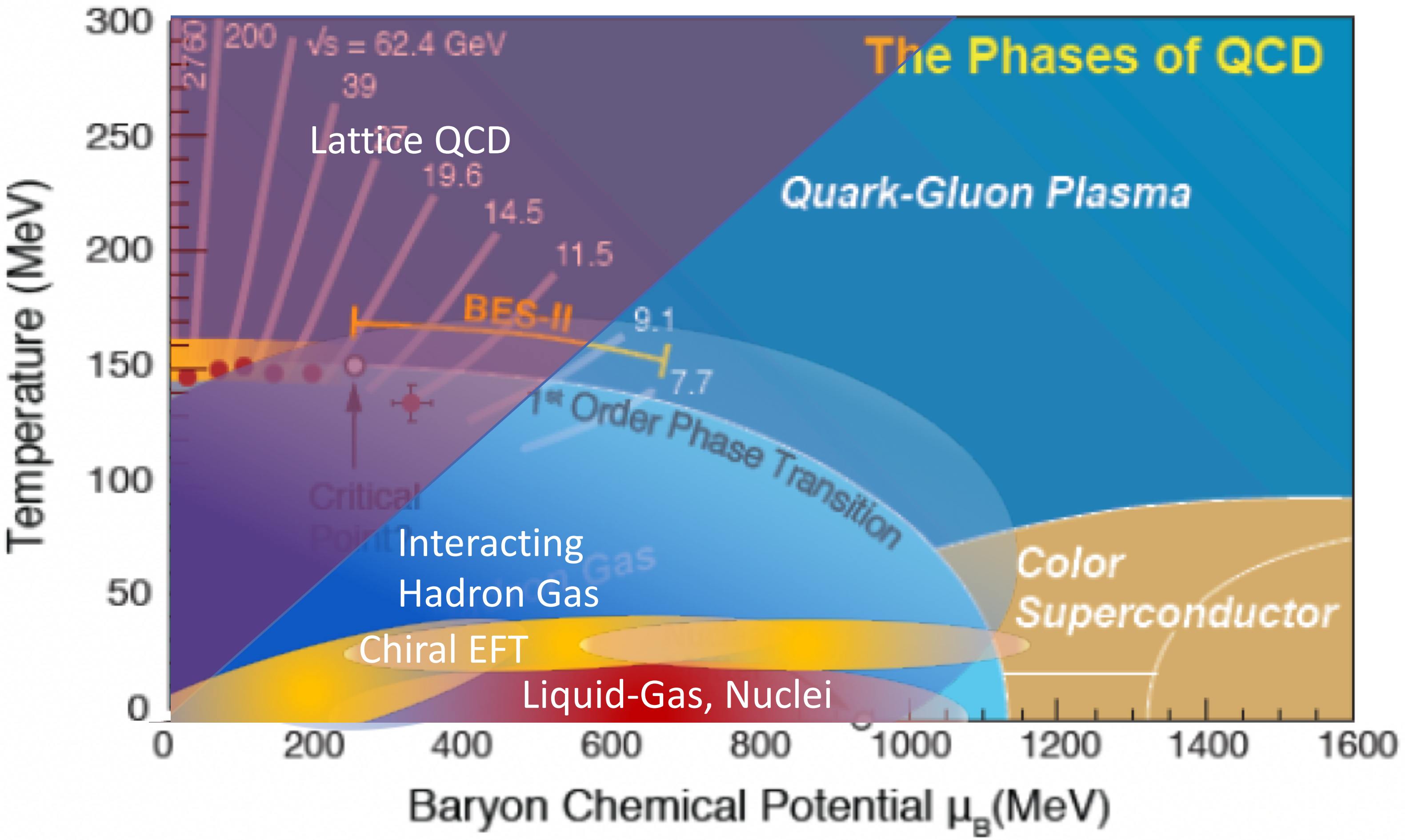

Lattice QCD: WB: PRL (2021)
Interacting HRG: V. Vovchenko et al., PRL (2017)
Liquid-gas, Nuclei: see e.g. Du et al. PRC (2019)
Chiral EFT: see e.g. Holt, Kaiser, PRD (2017)

What happens at large densities?

- We need to merge the lattice QCD equation of state with other effective theories
- Careful study of their respective range of validity
- Constrain the parameters to reproduce known limits
- Test different possibilities and validate/exclude them

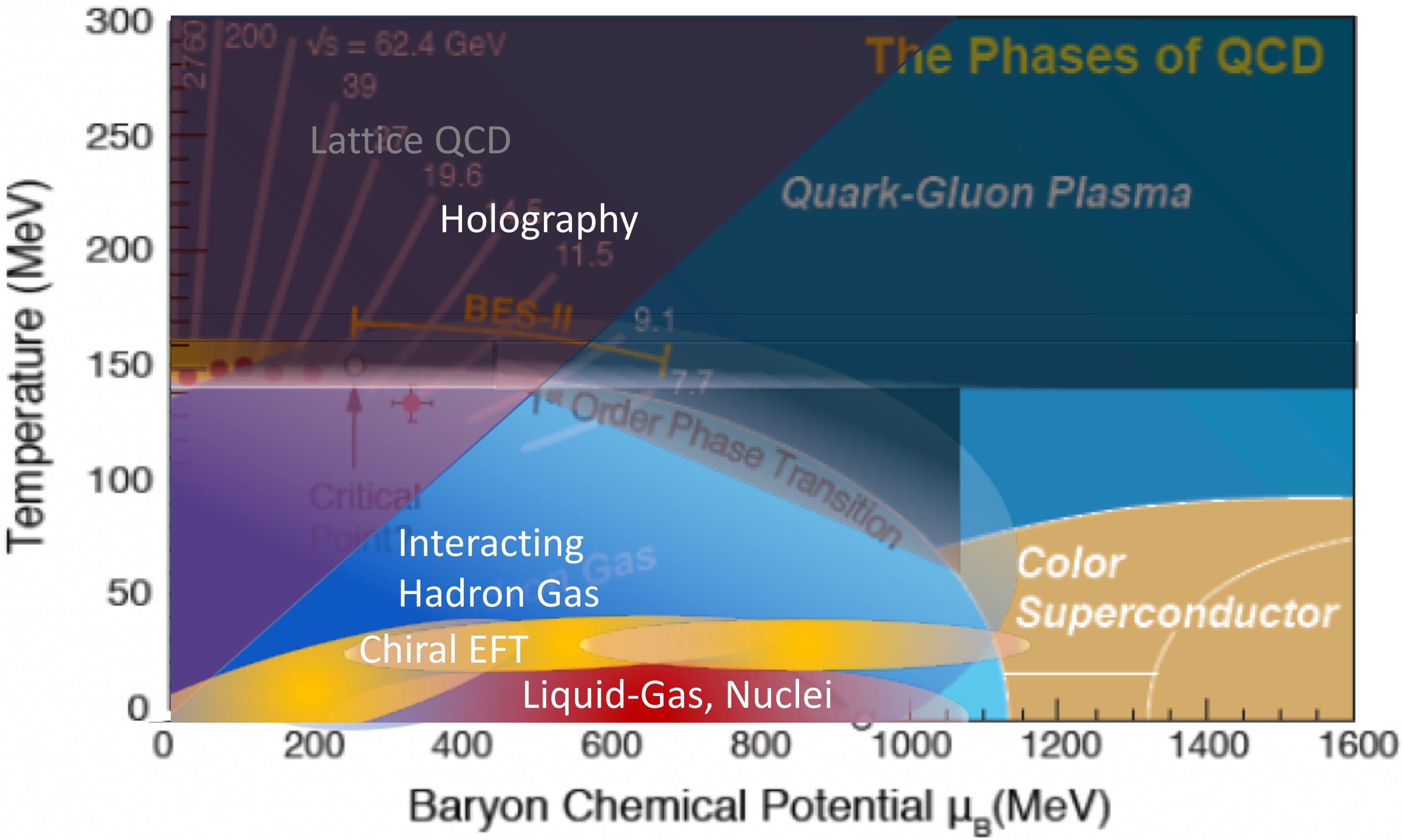

Lattice QCD: WB: PRL (2021)
Interacting HRG: V. Vovchenko et al., PRL (2017)
Liquid-gas, Nuclei: see e.g. Du et al. PRC (2019)
Chiral EFT: see e.g. Holt, Kaiser, PRD (2017)
Holography: see e.g. R. Critelli et al., PRD (2017)

What happens at large densities?

- We need to merge the lattice QCD equation of state with other effective theories
- Careful study of their respective range of validity
- Constrain the parameters to reproduce known limits
- Test different possibilities and validate/exclude them

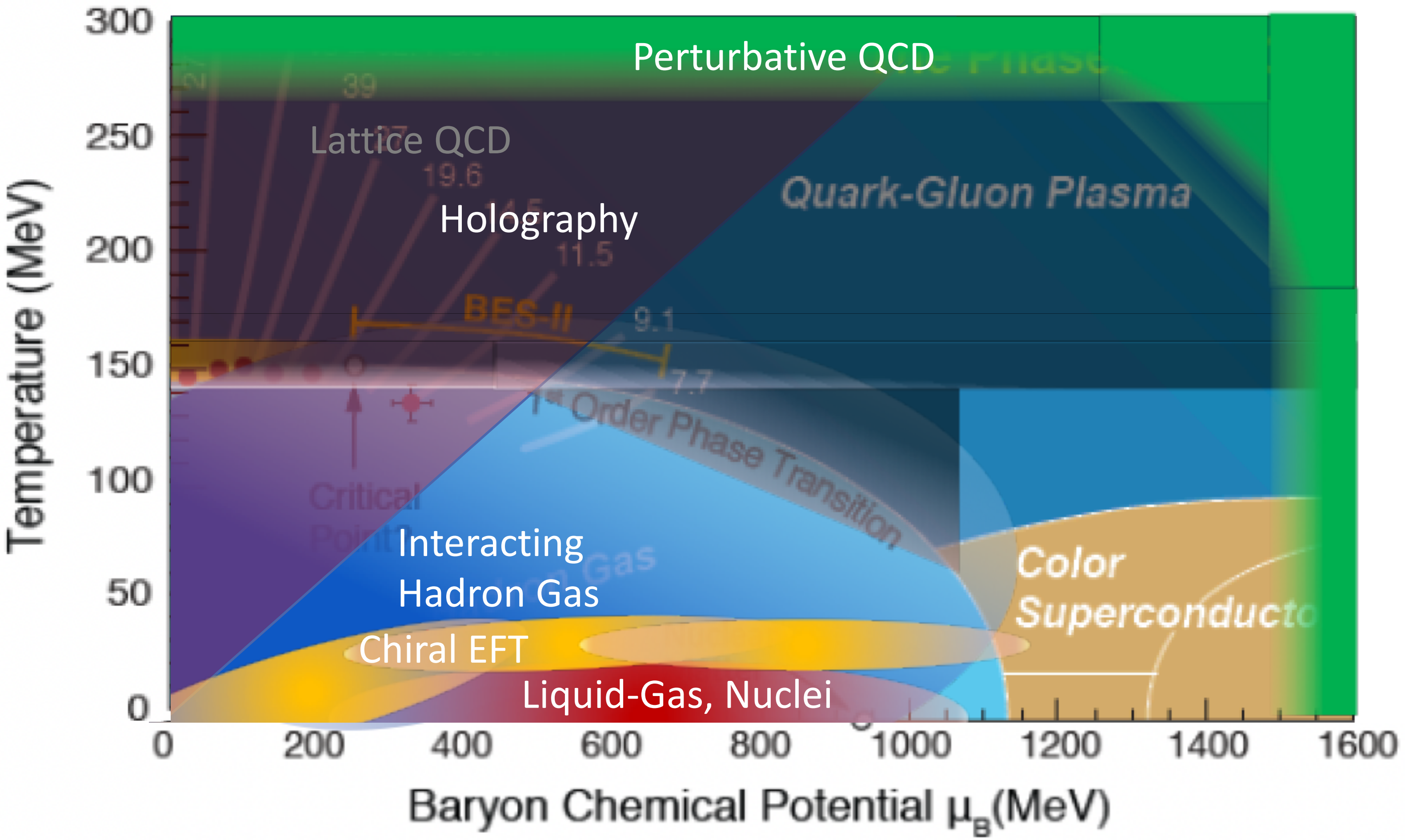

Lattice QCD: WB: PRL (2021)
Interacting HRG: V. Vovchenko et al., PRL (2017)
Liquid-gas, Nuclei: see e.g. Du et al. PRC (2019)
Chiral EFT: see e.g. Holt, Kaiser, PRD (2017)
Holography: see e.g. R. Critelli et al., PRD (2017)
pQCD: Andersen et al., PRD (2002); Annala et al., Nat. Ph. (2020)

What happens at large densities?

- We need to merge the lattice QCD equation of state with other effective theories
- Careful study of their respective range of validity
- Constrain the parameters to reproduce known limits
- Test different possibilities and validate/exclude them

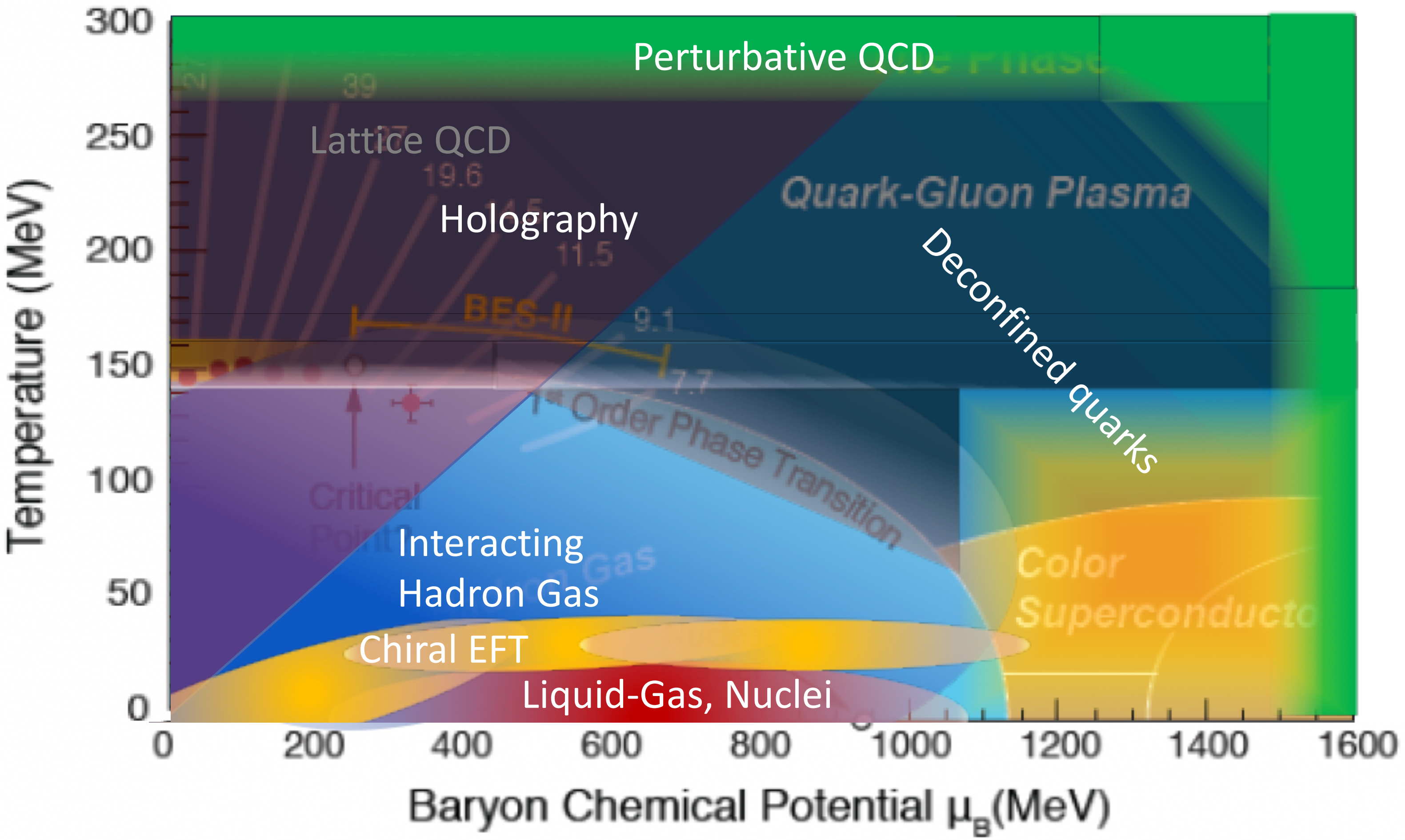

Lattice QCD: WB: PRL (2021)
Interacting HRG: V. Vovchenko et al., PRL (2017)
Liquid-gas, Nuclei: see e.g. Du et al. PRC (2019)
Chiral EFT: see e.g. Holt, Kaiser, PRD (2017)
Holography: see e.g. R. Critelli et al., PRD (2017)
pQCD: Andersen et al., PRD (2002); Annala et al., Nat. Ph. (2020)
quarks: Dexheimer et al., PRC (2009); Baym et al., Astr. J. (2019)

What happens at large densities?

- We need to merge the lattice QCD equation of state with other effective theories
- Careful study of their respective range of validity
- Constrain the parameters to reproduce known limits
- Test different possibilities and validate/exclude them

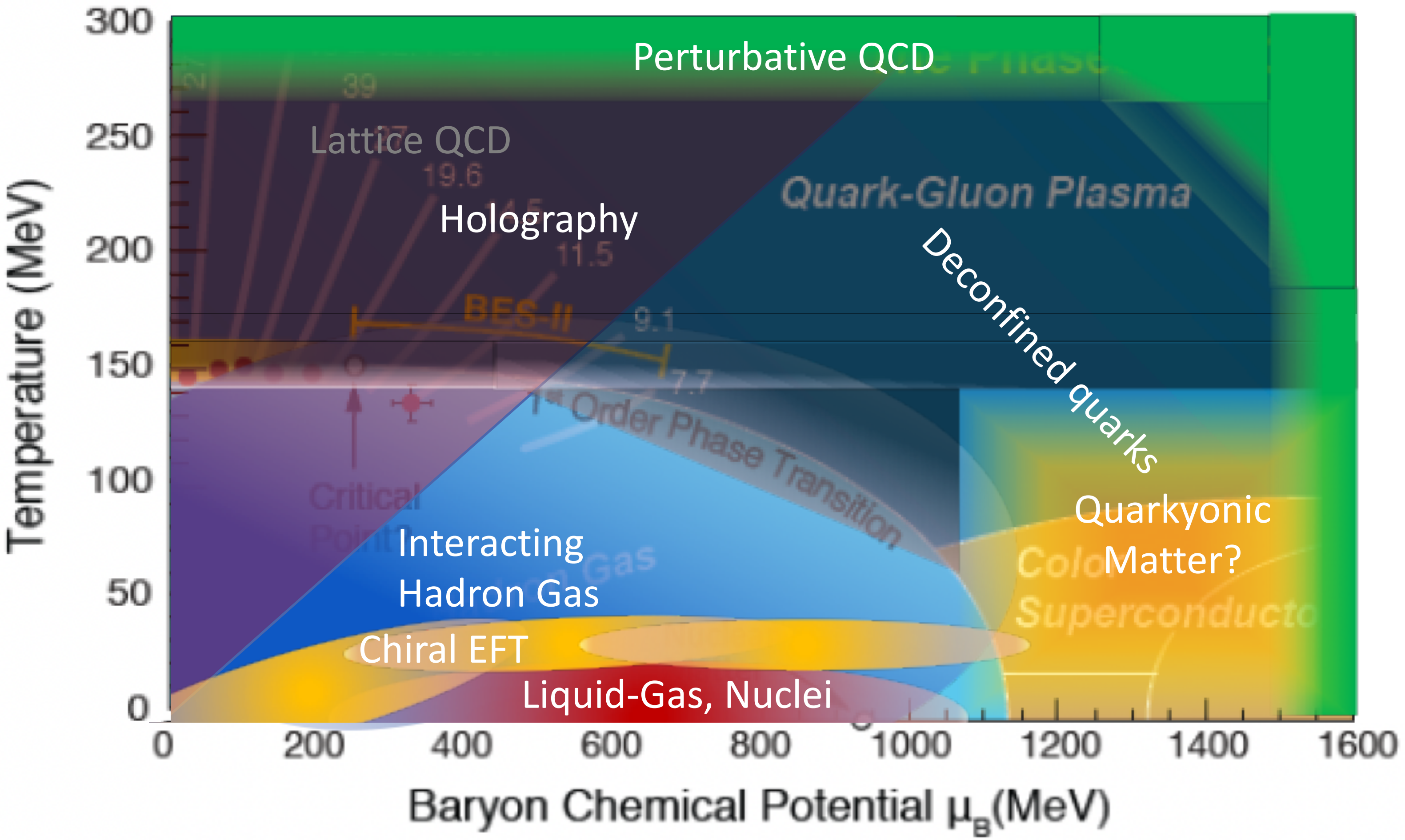

Lattice QCD: WB: PRL (2021)
Interacting HRG: V. Vovchenko et al., PRL (2017)
Liquid-gas, Nuclei: see e.g. Du et al. PRC (2019)
Chiral EFT: see e.g. Holt, Kaiser, PRD (2017)
Holography: see e.g. R. Critelli et al., PRD (2017)

pQCD: Andersen et al., PRD (2002); Annala et al., Nat. Ph. (2020)
quarks: Dexheimer et al., PRC (2009); Baym et al., Astr. J. (2019)
quarkyonic: McLerran, Pisarski NPA (2007)

What happens at large densities?

- We need to merge the lattice QCD equation of state with other effective theories
- Careful study of their respective range of validity
- Constrain the parameters to reproduce known limits
- Test different possibilities and validate/exclude them

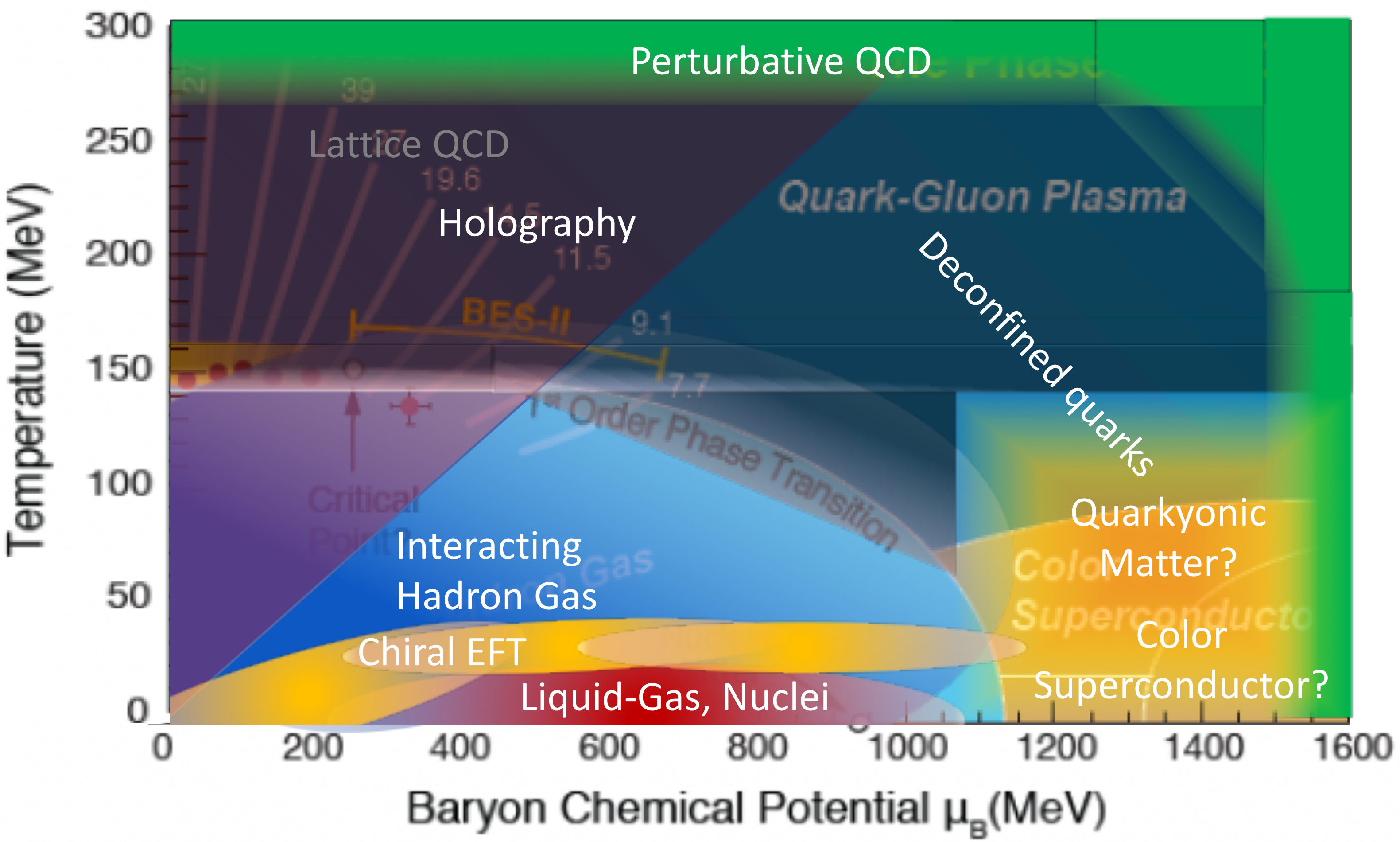

Lattice QCD: WB: PRL (2021)
Interacting HRG: V. Vovchenko et al., PRL (2017)
Liquid-gas, Nuclei: see e.g. Du et al. PRC (2019)
Chiral EFT: see e.g. Holt, Kaiser, PRD (2017)
Holography: see e.g. R. Critelli et al., PRD (2017)

pQCD: Andersen et al., PRD (2002); Annala et al., Nat. Ph. (2020)
quarks: Dexheimer et al., PRC (2009); Baym et al., Astr. J. (2019)
quarkyonic: McLerran, Pisarski NPA (2007)
CSC: Alford et al., PLB (1998); Rapp et al., PRL (1998).

Modular Unified Solver of the Equation of State collaboration

- Funded by NSF through CSSI program
- Developers and Users are working together to create a sustainable software to generate equations of state in the whole phase space
- Modular: Different models (``modules”) to describe the EoS in different regimes of phase space
- Unified: Modules smoothly integrated to (i) ensure maximal coverage of phase space, and (ii) respects constraints

muses

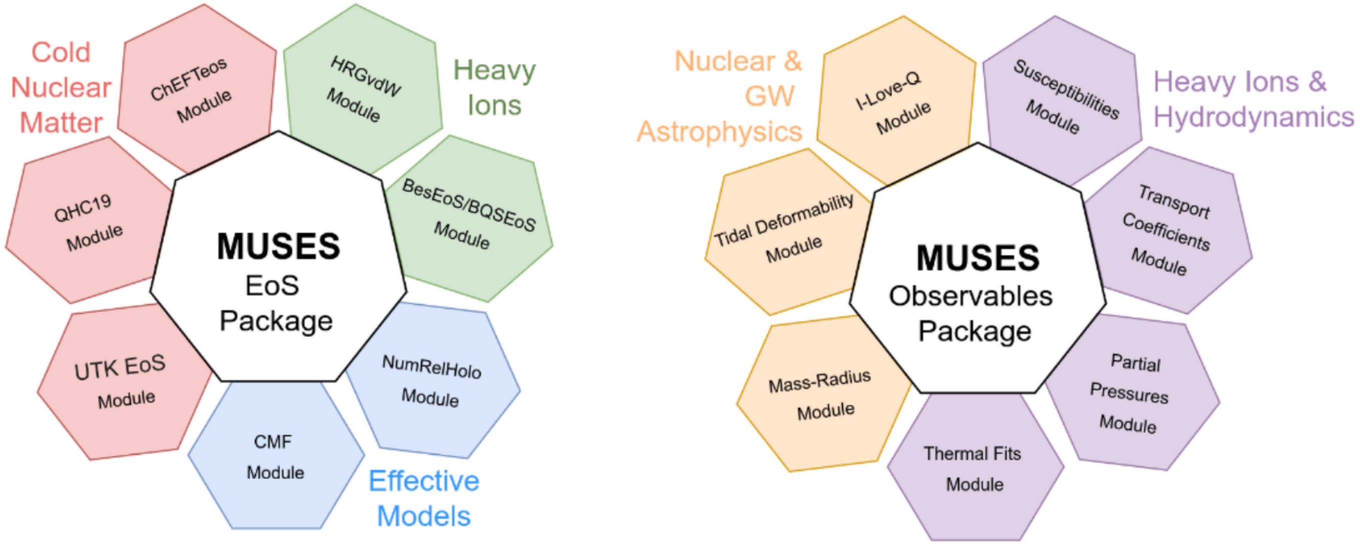

Conclusions

- Need for quantitative results at finite-density to support the experimental programs and reach out to the Neutron Star merger regime
- Current lattice results for thermodynamics available up to $\mu_B/T \leq 3.5$
- Extensions to higher densities by means of effective theories

Novel expansion method

WB, PRL (2021)

Observation: the temperature-dependence of baryonic density

$$n_B(T)/\hat{\mu}_B = \chi_1^B(T,\hat{\mu}_B)/\hat{\mu}_B$$

at finite imaginary chemical potential is just a shift in temperature from the $\mu_B = 0$ results for χ_2^B :

$$\frac{\chi_1^B(T,\hat{\mu}_B)}{\hat{\mu}_B} = \chi_2^B(T',0) \ ,$$

$$T'(T,\hat{\mu}_B) = T\left(1 + \kappa_2^{BB}(T)\hat{\mu}_B^2 + \kappa_4^{BB}(T)\hat{\mu}_B^4 + \mathcal{O}(\hat{\mu}_B^6)\right)$$

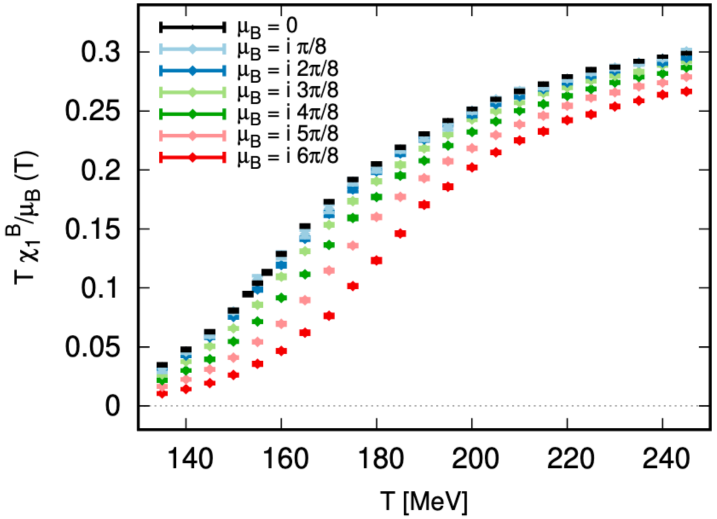

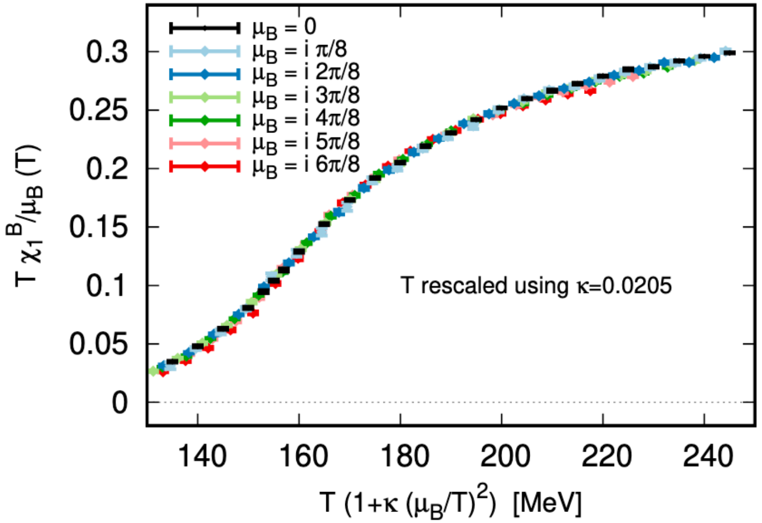

Results for the coefficients

S. Borsanyi, C. R. et al., PRL (2021)

Our initial guess was not far-off:

- Fairly constant $\kappa_2(T)$ over a large T-range
- Clear separation in magnitude between $\kappa_2(T)$ and $\kappa_4(T)$ hints at better convergence
- Agreement with the HRG model results at low temperatures
- Polynomial fits of $\kappa_2(T)$ and $\kappa_4(T)$ before use in thermodynamics (good fit qualities)

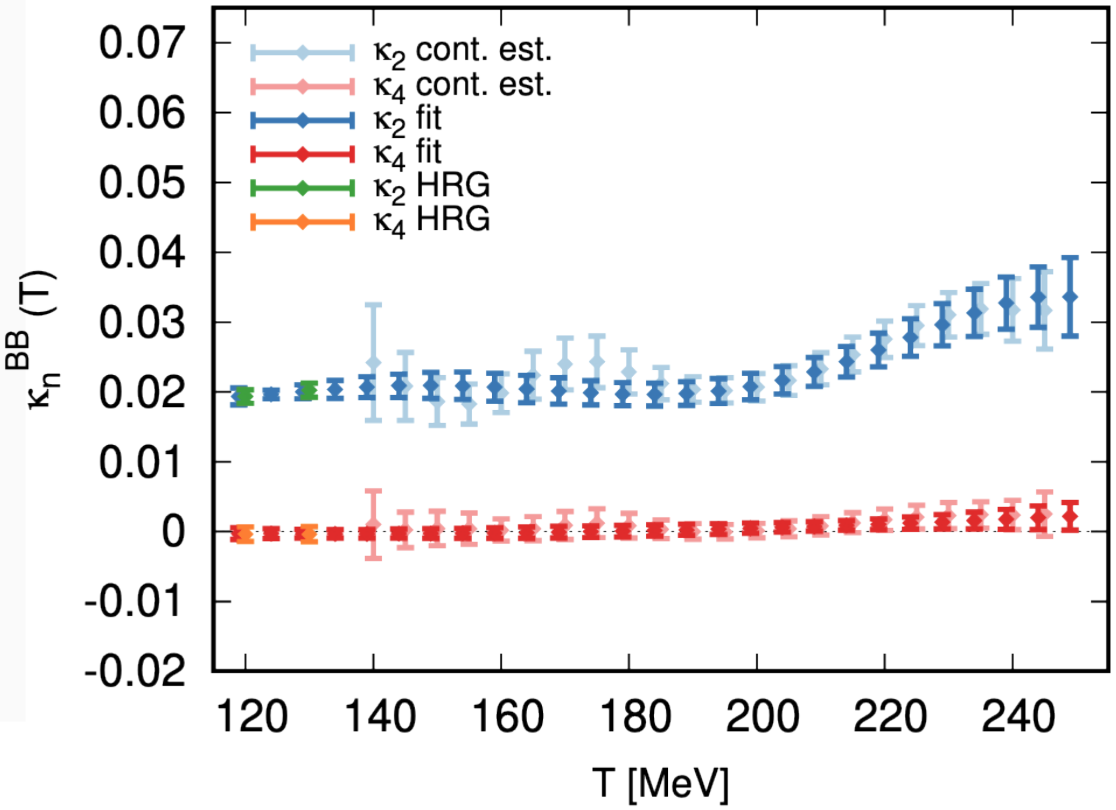

Novel expansion method

Once n_B is determined, we have everything we need to extract the other quantities

$$\frac{p(\mu_B,T)}{T^4} = \hat{p}(\hat{\mu}_B,T) = \hat{p}(0,T) + \int_0^{\hat{\mu}_B} \mathrm{d}\hat{\mu}'_B\, \hat{n}_B(\hat{\mu}'_B,T) \qquad s(\mu_B,T) = \left.\frac{\partial p(\mu_B,T)}{\partial T}\right|_{\mu}$$

WB, PRL (2021)

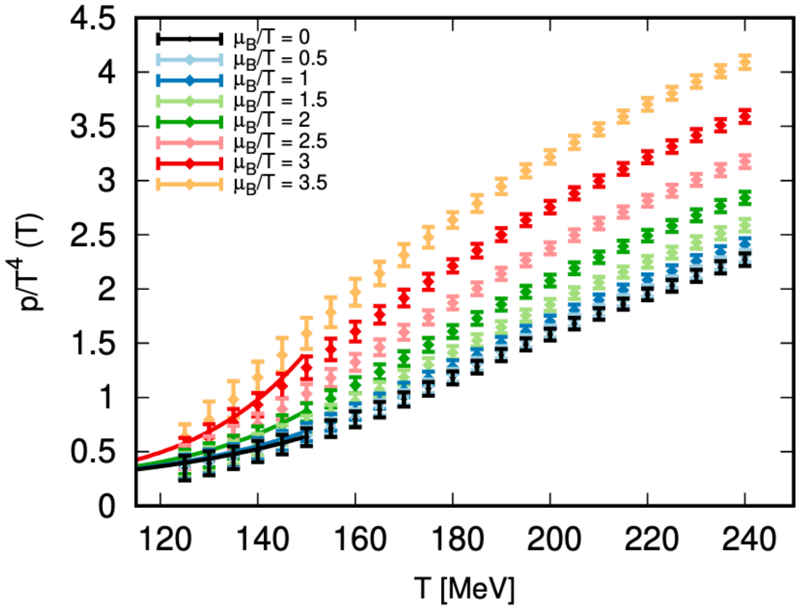

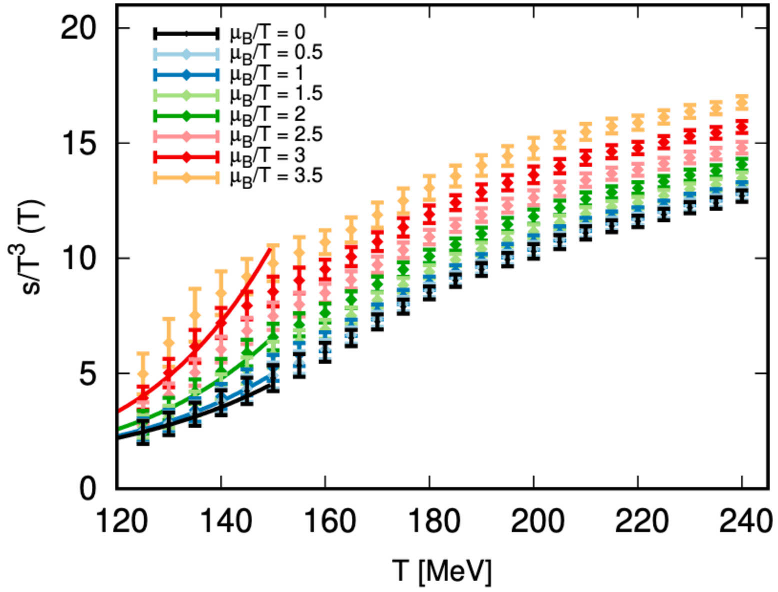

How can lattice QCD support the experiments?

Equation of state
- Needed for hydrodynamic description of the QGP

QCD phase diagram
- Transition line at finite density
- Constraints on the location of the critical point

Fluctuations of conserved charges
- Can be simulated on the lattice and measured in experiments
- Can give information on the evolution of heavy-ion collisions
- Can give information on the critical point

Formulation

S. Borsanyi, C. R. et al., PRL (2021)

- We have observed the $\hat{\mu}_B$-dependence seems to amount to a simple T- rescaling
- A simplistic scenario with a single T- independent parameter κ does not provide a systematic treatment which can serve as an alternative expansion scheme
- We allow for more than $\mathcal{O}(\hat{\mu}^2)$ expansion of T' and let the coefficients be $T-$dependent:

$$\frac{\chi_1^B(T,\hat{\mu}_B)}{\hat{\mu}_B} = \chi_2^B(T',0)\ , \quad T' = T\left(1+\kappa_2(T)\,\hat{\mu}_B^2+\kappa_4(T)\,\hat{\mu}_B^4+\mathcal{O}(\hat{\mu}_B^6)\right)$$

- **Important:** we are simply re-organizing the Taylor expansion via an expansion in the shift

$$\Delta T = T - T' = \left(\kappa_2(T)\,\hat{\mu}_B^2+\kappa_4(T)\,\hat{\mu}_B^4+\mathcal{O}(\hat{\mu}_B^6)\right)$$

- Comparing the (Taylor) expansion in $\hat{\mu}_B$ and our expansion in ΔT order by order, we can relate $\chi_n^B(T)$ and $\kappa_n(T)$

QCD phase diagram

TRANSITION TEMPERATURE

TRANSITION LINE

TRANSITION WIDTH

QCD matter under extreme conditions

To address these questions, we need fundamental theory and experiment

Theory: Quantum Chromodynamics

- QCD is the fundamental theory of strong interactions
- It describes interactions among quarks and gluons

$$L_{QCD} = \sum_{i=1}^{n_f} \overline{\psi}_i \gamma_\mu \left(i\partial^\mu - g A_a^\mu \frac{\lambda_a}{2} \right) \psi_i - m_i \overline{\psi}_i \psi_i - \frac{1}{4} \sum_a F_a^{\mu\nu} F_a^{\mu\nu}$$

$$F_a^{\mu\nu} = \partial^\mu A_a^\nu - \partial^\nu A_a^\mu + i f_{abc} A_b^\mu A_c^\mu$$

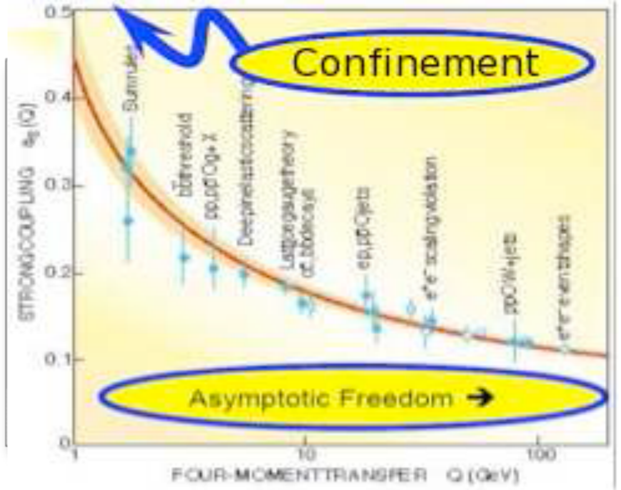

Experiment: heavy-ion collisions

- Quark-Gluon Plasma (QGP) discovery at RHIC and LHC:
- SURPRISE!!! QGP is a PERFECT FLUID
- Changes our idea of QGP (no weak coupling)
- Microscopic origin still unknown

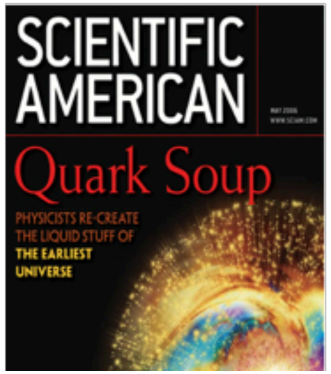

Phase Diagram from Lattice QCD

The transition at μ_B=0 is a smooth crossover

Aoki et al., Nature (2006)
Borsanyi et al., JHEP (2010)
Bazavov et al., PRD (2012)

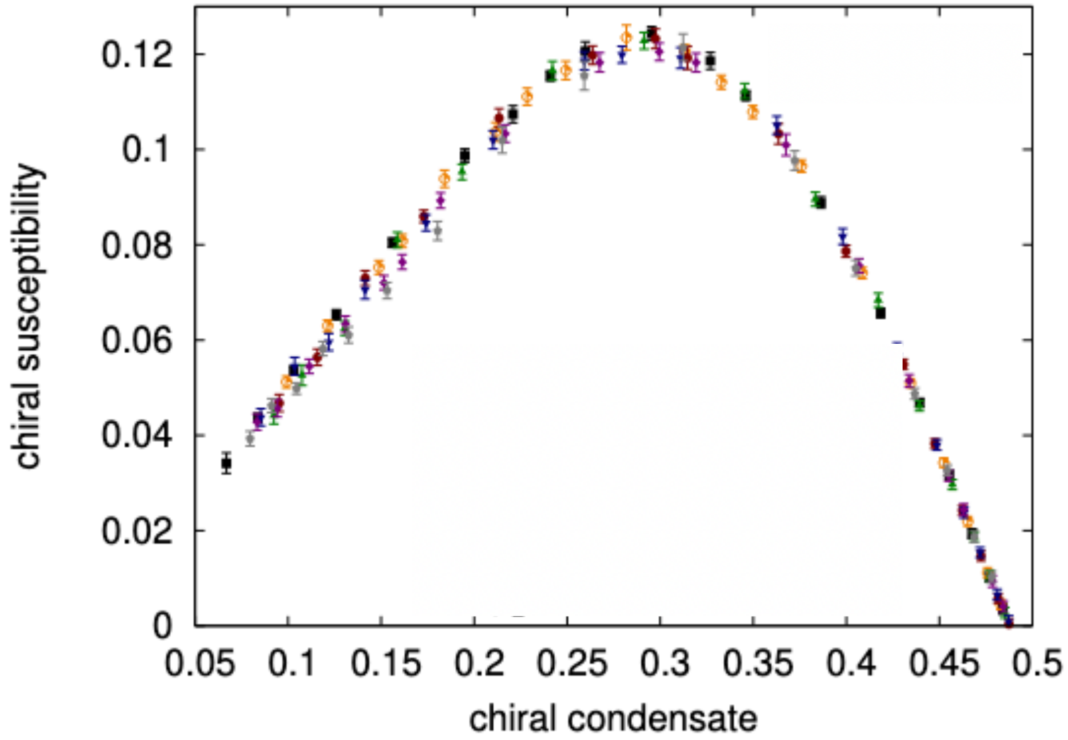

QCD transition temperature and curvature

$$\frac{T_c(\mu_B)}{T_0} = 1 - \kappa_2 \left(\frac{\mu_B}{T_0}\right)^2 - \kappa_4 \left(\frac{\mu_B}{T_0}\right)^4 + \mathcal{O}(\mu_B^6)$$

Borsanyi, C. R. et al. PRL (2020)

- Latest results on T_O from WB collaboration based on subtracted chiral condensate and chiral susceptibility

T_O=158.0±0.6 MeV

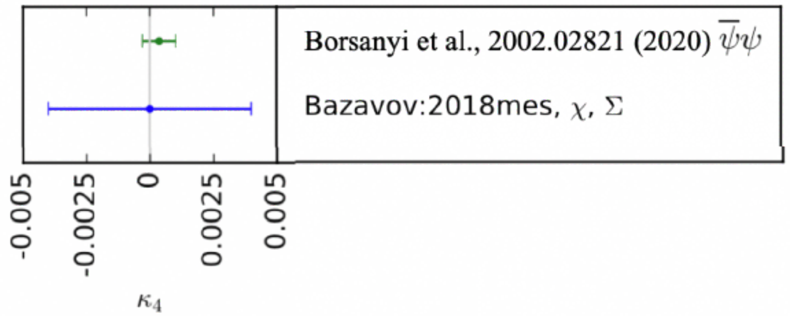

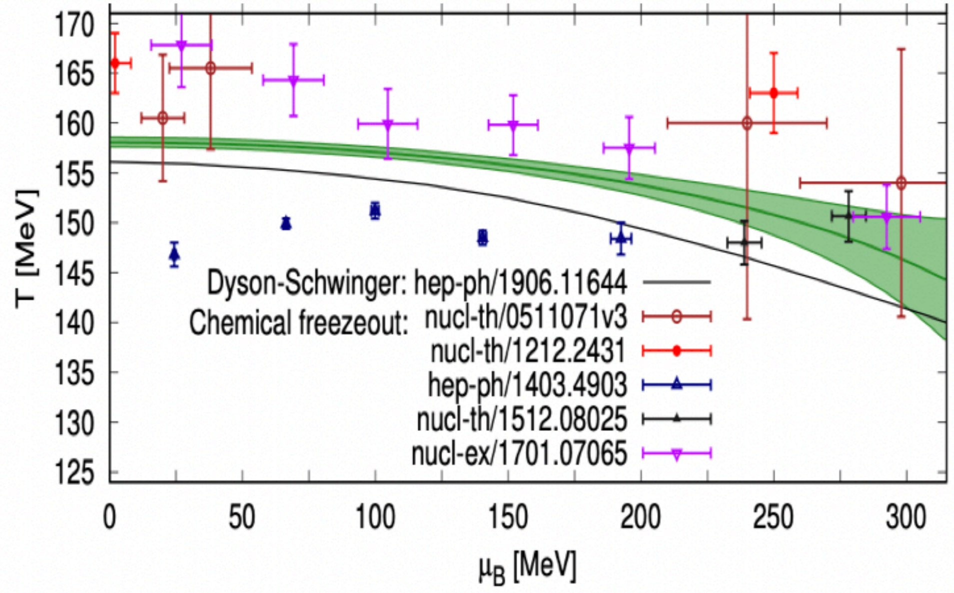

$$\kappa_2 = 0.0153 \pm 0.0018 \,, \quad \kappa_4 = 0.00032 \pm 0.00067$$

Limit on the location of the critical point

For a genuine phase transition, the height of the peak of the chiral susceptibility diverges and the width shrinks to zero

Height of chiral susceptibility peak

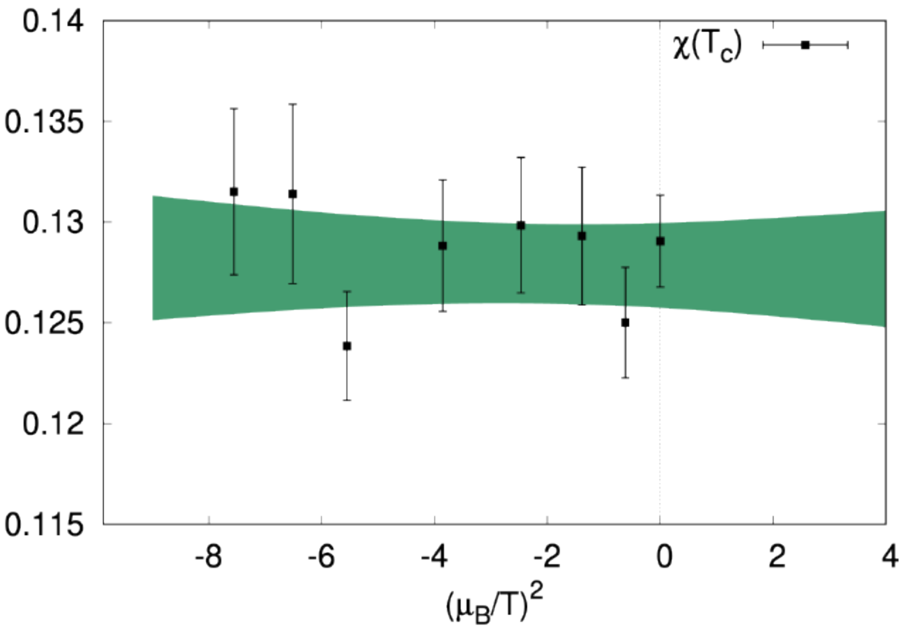

Width of chiral susceptibility peak

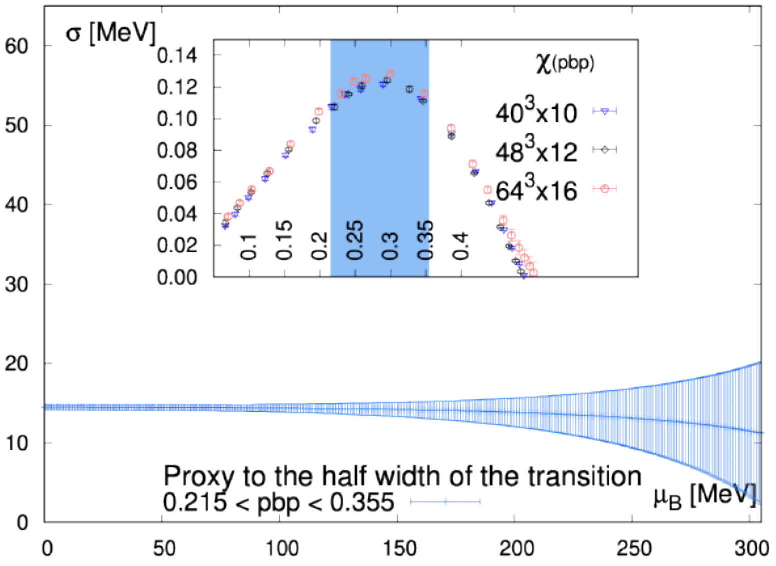

No sign of criticality for μ_B<300 MeV

Borsanyi, C. R. et al. PRL (2020)

Fluctuations of conserved charges

COMPARISON TO EXPERIMENT

CHEMICAL FREEZE-OUT PARAMETERS

Fluctuations of conserved charges

Definition:

$$\chi^{BSQ}_{lmn} = \frac{\partial^{\,l+m+n} p/T^4}{\partial(\mu_B/T)^l \partial(\mu_S/T)^m \partial(\mu_Q/T)^n}.$$

Relationship between chemical potentials:

$$\begin{aligned}
\mu_u &= \frac{1}{3}\mu_B + \frac{2}{3}\mu_Q; \\
\mu_d &= \frac{1}{3}\mu_B - \frac{1}{3}\mu_Q; \\
\mu_s &= \frac{1}{3}\mu_B - \frac{1}{3}\mu_Q - \mu_S.
\end{aligned}$$

They can be calculated on the lattice and compared to experiment

Evolution of a heavy-ion collision

- Chemical freeze-out: inelastic reactions cease: the chemical composition of the system is fixed (particle yields and fluctuations)
- Kinetic freeze-out: elastic reactions cease: spectra and correlations are frozen (free streaming of hadrons)
- Hadrons reach the detector

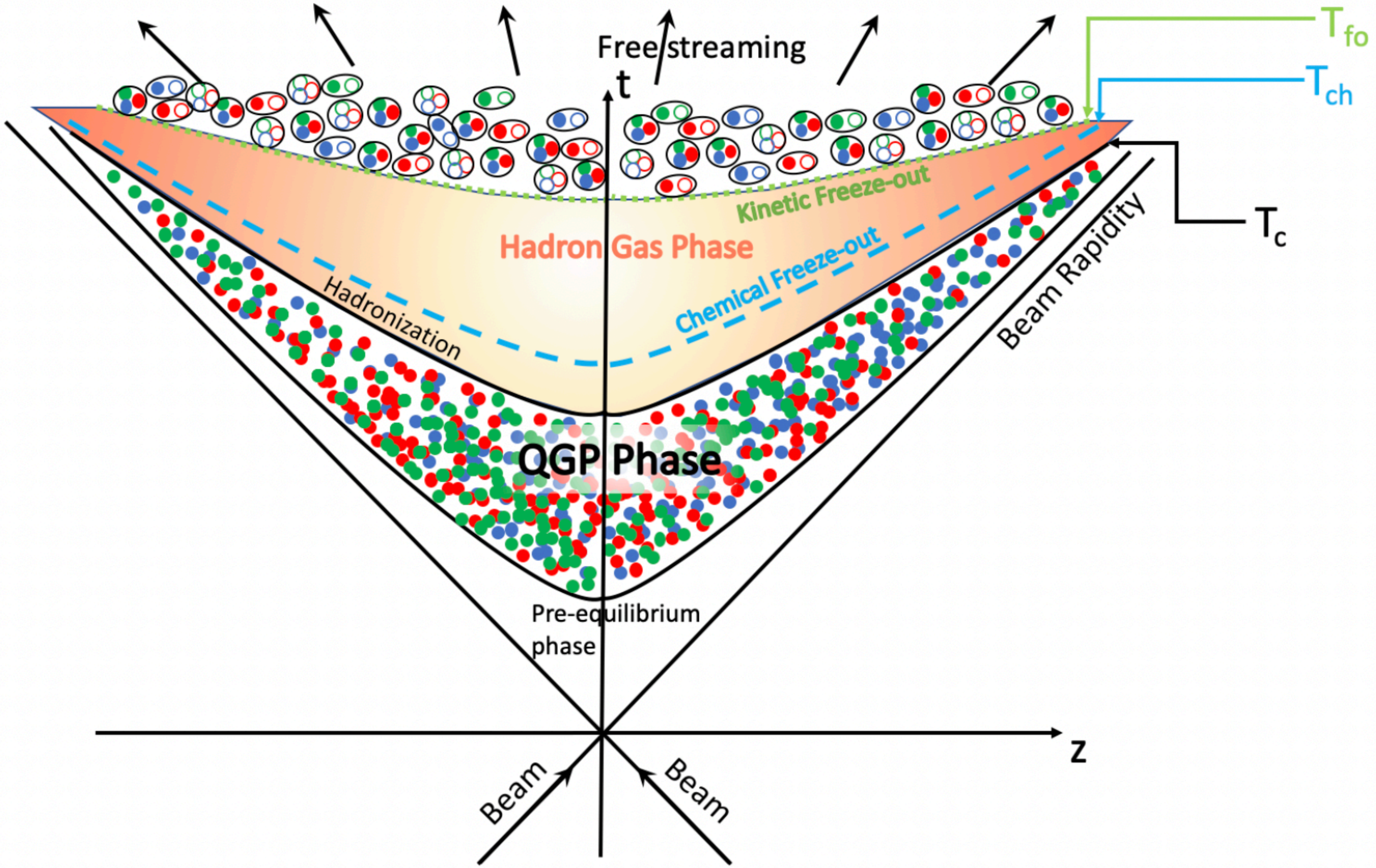

Evolution of a heavy-ion collision

- Chemical freeze-out: inelastic reactions cease: the chemical composition of the system is fixed (particle yields and fluctuations)
- Kinetic freeze-out: elastic reactions cease: spectra and correlations are frozen (free streaming of hadrons)
- Hadrons reach the detector

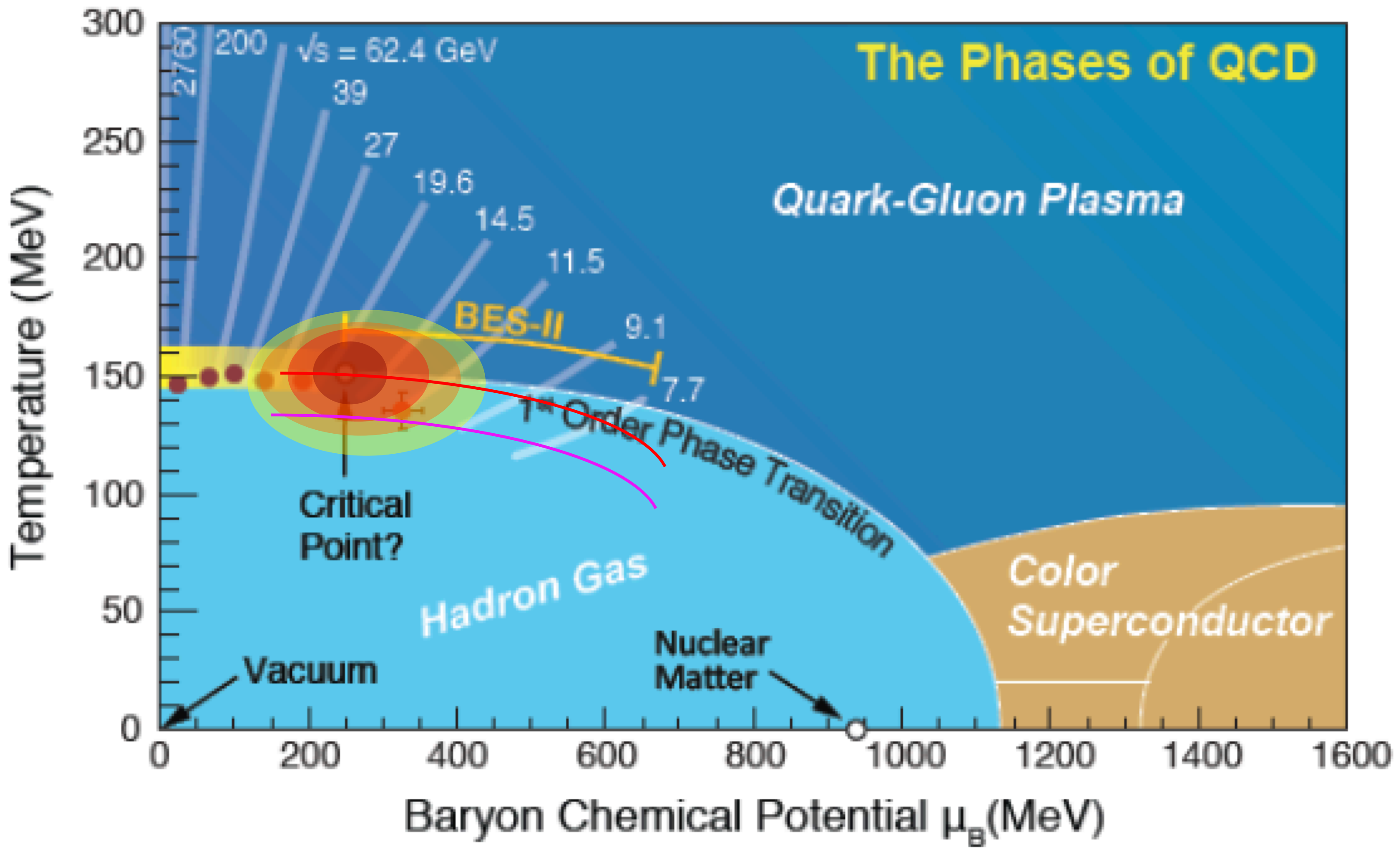

Connection to experiment

- Consider the number of electrically charged particles N_Q
- Its average value over the whole ensemble of events is $\langle N_Q \rangle$
- In experiments it is possible to measure its event-by-event distribution

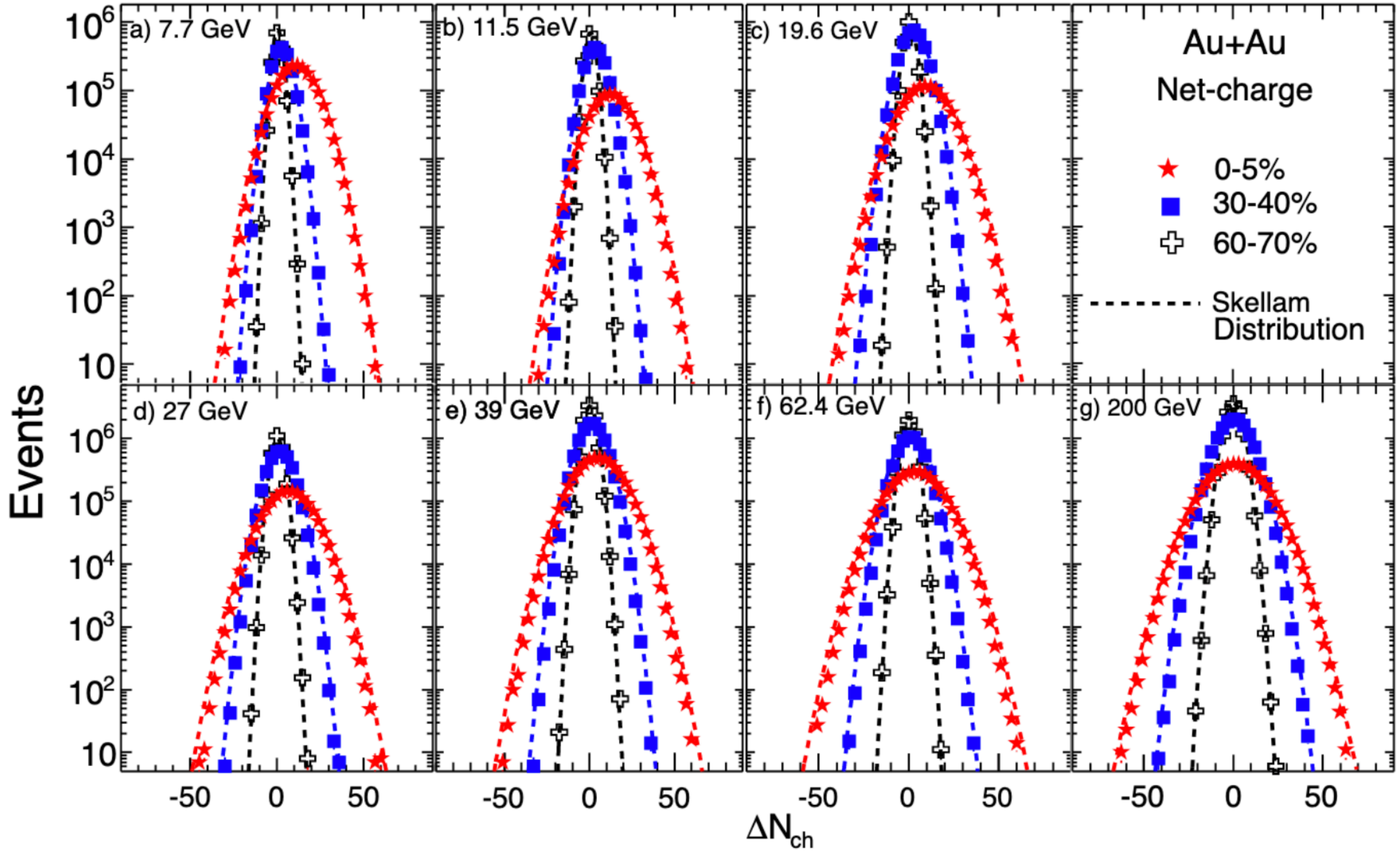

STAR Collab., PRL (2014)

Connection to experiment

Fluctuations of conserved charges are the cumulants of their event-by-event distribution

$$\text{mean}: \; M = \chi_1 \qquad \text{variance}: \; \sigma^2 = \chi_2$$

$$\text{skewness}: \; S = \chi_3/\chi_2^{3/2} \qquad \text{kurtosis}: \; \kappa = \chi_4/\chi_2^2$$

$$S\sigma = \chi_3/\chi_2 \qquad \kappa\sigma^2 = \chi_4/\chi_2$$

$$M/\sigma^2 = \chi_1/\chi_2 \qquad S\sigma^3/M = \chi_3/\chi_1$$

F. Karsch: Centr. Eur. J. Phys. (2012)

The chemical potentials are not independent: fixed to match the experimental conditions:

$\langle n_S \rangle = 0$ $\langle n_Q \rangle = 0.4 \langle n_B \rangle$

Freeze-out line from first principles

Use T- and μ_B-dependence of R_{12}^Q and R_{12}^B for a combined fit:

$$R^Q_{12}(T,\mu_B) = \frac{\chi^Q_1(T,\mu_B)}{\chi^Q_2(T,\mu_B)} = \frac{\chi^{QB}_{11}(T,0) + \chi^Q_2(T,0)q_1(T) + \chi^{QS}_{11}(T,0)s_1(T)}{\chi^Q_2(T,0)}\frac{\mu_B}{T} + \mathcal{O}(\mu_B^3).$$

$$R^B_{12}(T,\mu_B) = \frac{\chi^B_1(T,\mu_B)}{\chi^B_2(T,\mu_B)} = \frac{\chi^B_2(T,0) + \chi^{BQ}_{11}(T,0)q_1(T) + \chi^{BS}_{11}(T,0)s_1(T)}{\chi^B_2(T,0)}\frac{\mu_B}{T} + \mathcal{O}(\mu_B^3)$$

WB: S. Borsanyi et al., in preparation

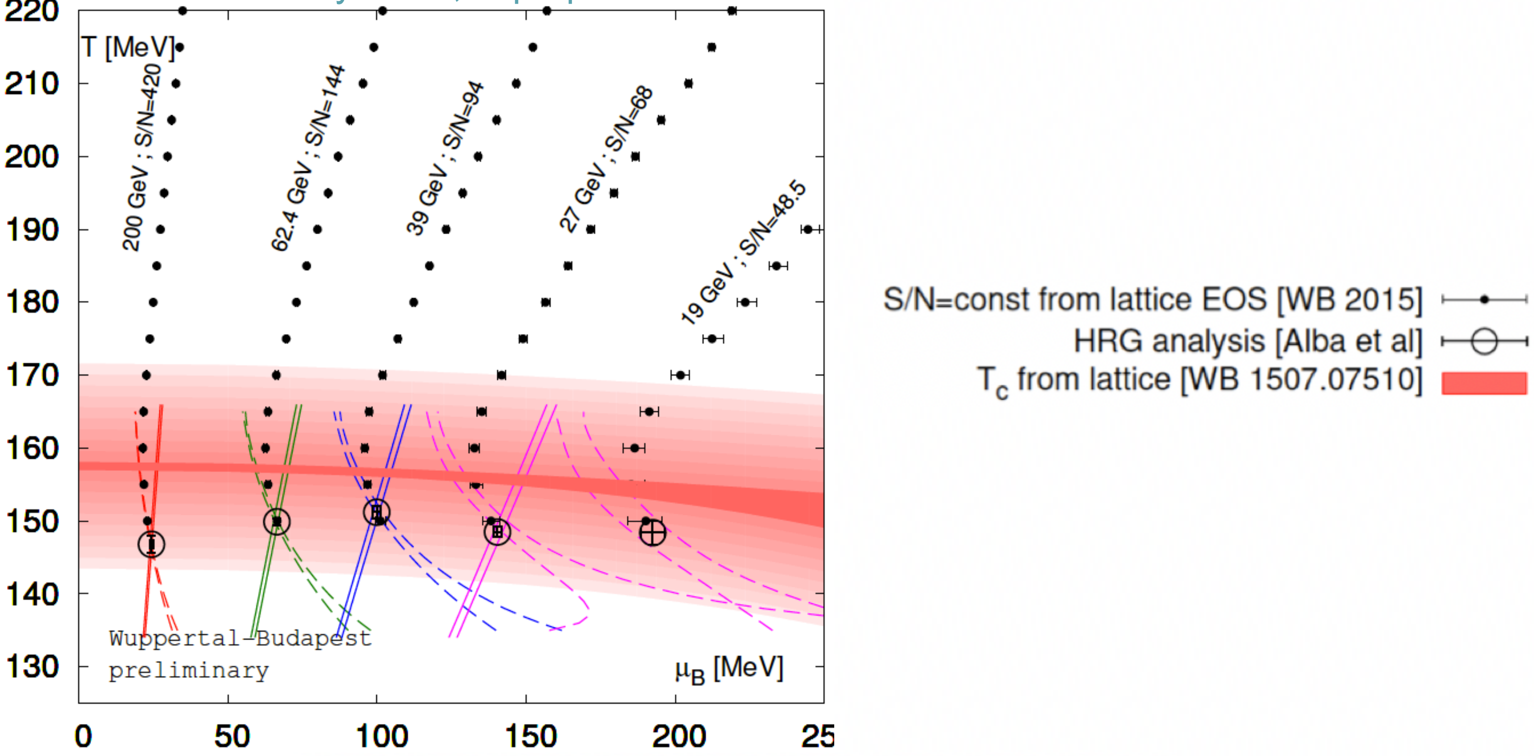

Conclusions

- Need for quantitative results at finite-density to support the experimental programs
  - Equation of state
  - Phase transition line
  - Fluctuations of conserved charges
- Current lattice results for thermodynamics up to $\mu_B/T \leq 3.5$
- Extensions to higher densities by means of lattice-based models
- No indication of Critical Point from lattice QCD in the explored μ_B range

Anatomy of a multi-messenger merger

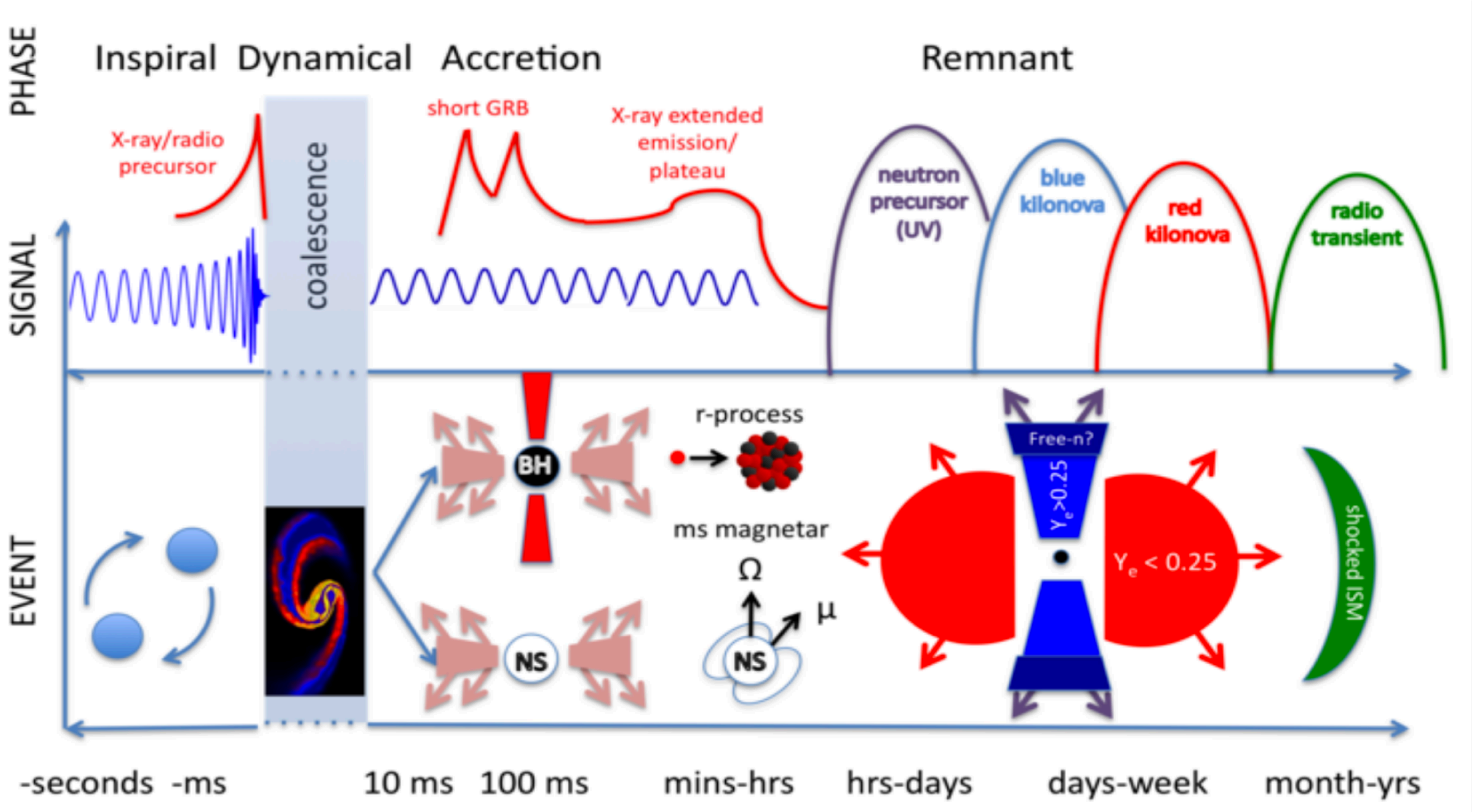

Fernandez & Metzger (2016)

Nuclear Physics is encoded in all phases!

Higher order fluctuations

$$\frac{S_B\sigma_B^3}{M_B} = \frac{\chi_3^B(T,\mu_B)}{\chi_1^B(T,\mu_B)} = \frac{\chi_4^B + s_1\chi_{31}^{BS} + q_1\chi_{31}^{BQ}}{\chi_2^B + s_1\chi_{11}^{BS} + q_1\chi_{11}^{BQ}} + \mathcal{O}(\mu_B^2) \equiv r_{31}^{B,0} + r_{31}^{B,2}\hat{\mu}_B^2 + \mathcal{O}(\mu_B^4)$$

$$\kappa_B\sigma_B^2 = \frac{\chi_4^B(T,\mu_B)}{\chi_2^B(T,\mu_B)} = \frac{\chi_4^B}{\chi_2^B} + \mathcal{O}(\mu_B^2) \equiv r_{42}^{B,0} + r_{42}^{B,2}\hat{\mu}_B^2 + \mathcal{O}(\mu_B^4)\ ,$$

WB, JHEP (2018)

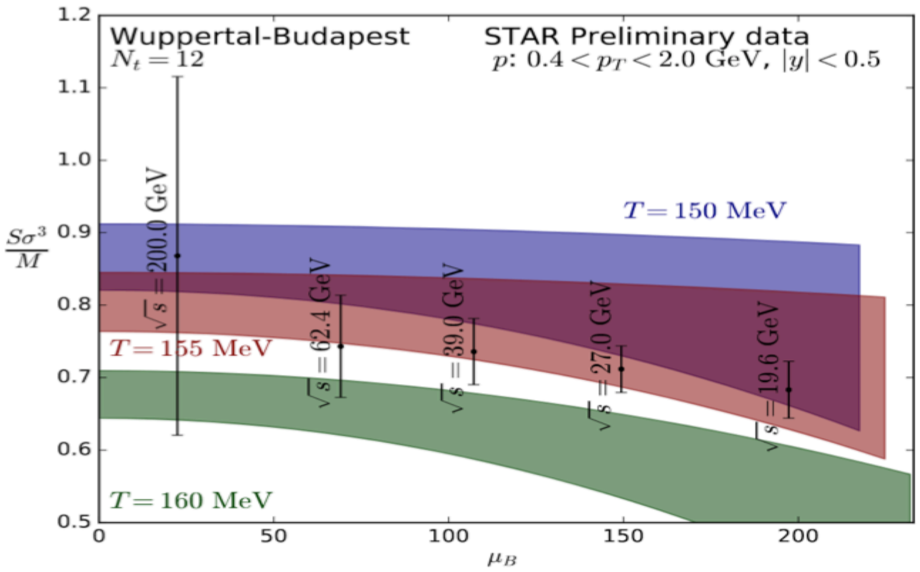

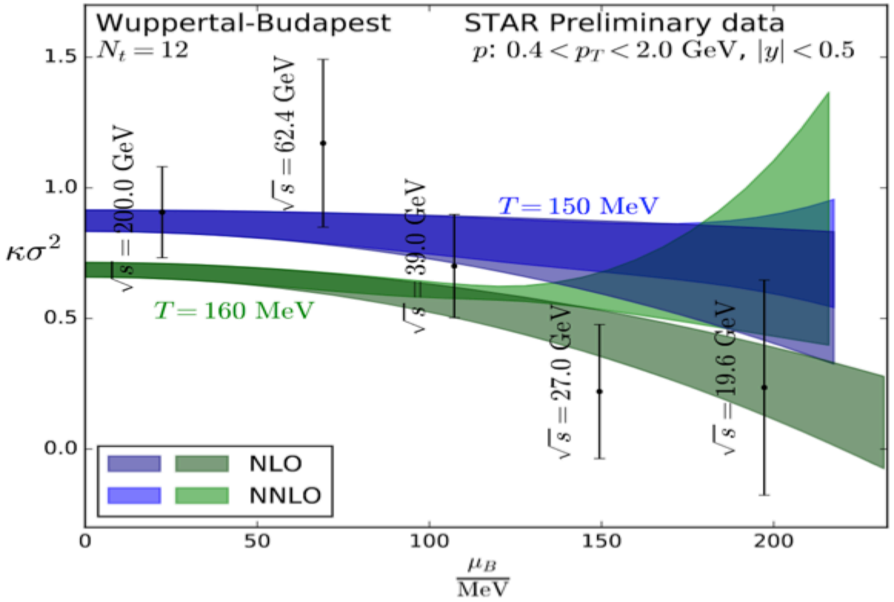

See also HotQCD, PRD (2017)

“Baryometer and Thermometer”

Let us look at the Taylor expansion of R^B_{31}

$$R^B_{31}(T,\mu_B) = \frac{\chi^B_3(T,\mu_B)}{\chi^B_1(T,\mu_B)} = \frac{\chi^B_4(T,0) + \chi^{BQ}_{31}(T,0)q_1(T) + \chi^{BS}_{31}(T,0)s_1(T)}{\chi^B_2(T,0) + \chi^{BQ}_{11}(T,0)q_1(T) + \chi^{BS}_{11}(T,0)s_1(T)} + \mathcal{O}(\mu_B^2)$$

- To order μ^2_B it is independent of μ_B: it can be used as a thermometer

- Let us look at the Taylor expansion of R^B_{12}

$$R^B_{12}(T,\mu_B) = \frac{\chi^B_1(T,\mu_B)}{\chi^B_2(T,\mu_B)} = \frac{\chi^B_2(T,0) + \chi^{BQ}_{11}(T,0)q_1(T) + \chi^{BS}_{11}(T,0)s_1(T)}{\chi^B_2(T,0)} \frac{\mu_B}{T} + \mathcal{O}(\mu_B^3)$$

- Once we extract T from R^B_{31}, we can use R^B_{12} to extract μ_B

The highest man-made temperature

LHC:
2012

5.5×10^{12} °C: 340.000 times the temperature at the center of the sun!!!

The produced energy density is 5 GeV/fm^3

In one year in America ~10^{20} J of energy are used

10^{20} J x 1eV/(1.6x10^{-19} J) = 6.6 x 10^{38} eV

At 5 GeV/fm^3 this would correspond to a volume:

$$6.6 \times 10^{38} eV \div \frac{5 \times 10^9 eV}{fm^3} = 1.3 \times 10^{29} fm^3$$

Or, equivalently, to a box of size:

$$\sqrt[3]{1.3 \times 10^{29} fm^3} = 5 \times 10^9 fm \times \frac{1m}{10^{15} fm} \times \frac{10^6 \mu m}{1m} = 5\mu m$$

Freeze-out parameters from B fluctuations

- Thermometer: $\frac{\chi_3^B(T,\mu_B)}{\chi_1^B(T,\mu_B)}$ $=S_B\sigma_B^3/M_B$ Baryometer: $\frac{\chi_1^B(T,\mu_B)}{\chi_2^B(T,\mu_B)}$ $=\sigma_B^2/M_B$

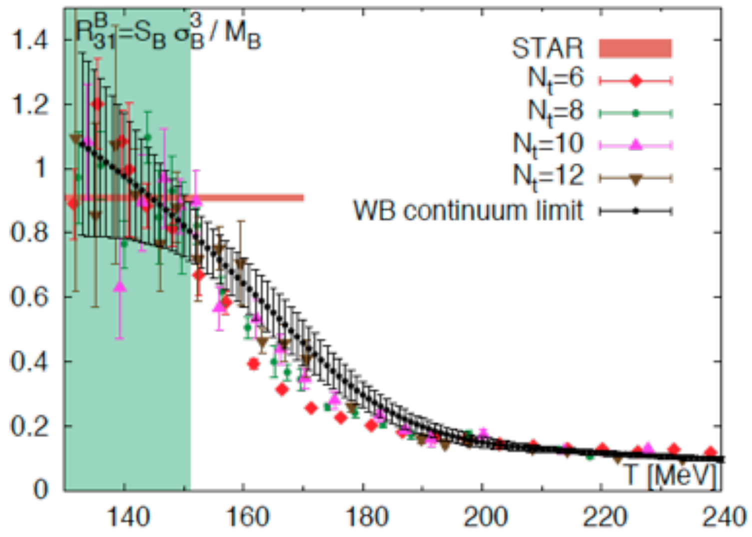

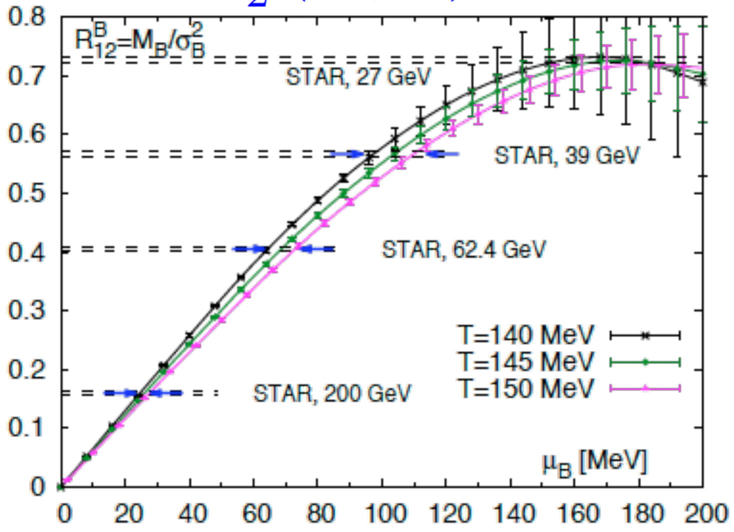

Upper limit: $T_f \leq 151\pm4$ MeV

WB: S. Borsanyi et al., PRL (2014)
STAR collaboration, PRL (2014)

Consistency between freeze-out chemical potential from electric charge and baryon number is found.

Pressure coefficients

<u>Simulations at imaginary μ_B:</u>

Continuum, O(10^4) configurations, errors include systematics (WB: NPA (2017)) **Strangeness neutrality**

c_2

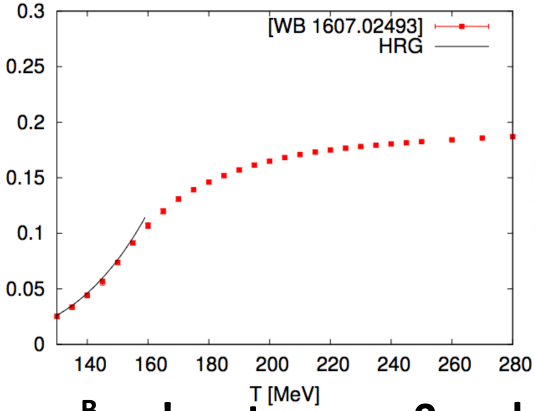

c_4

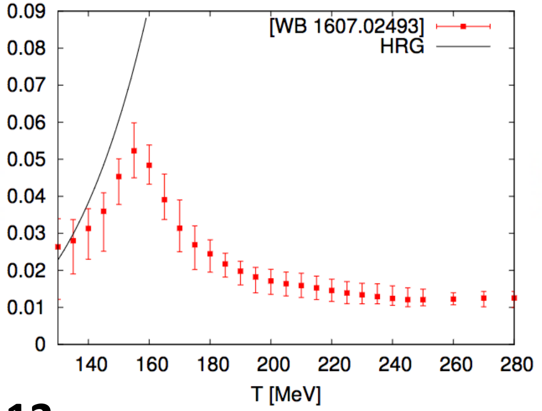

c_6

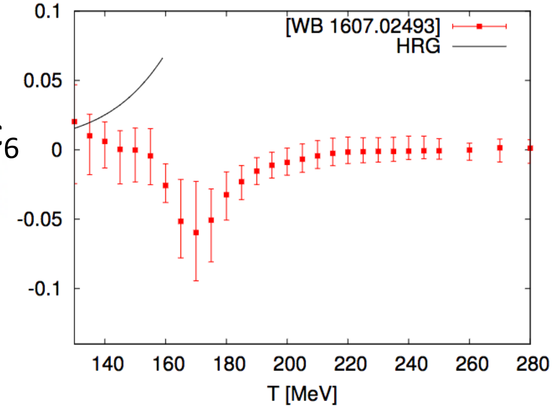

Results for $\chi_n^B = n!c_n$ at $\mu_S=\mu_Q=0$ and Nt=12

WB, JHEP (2018)

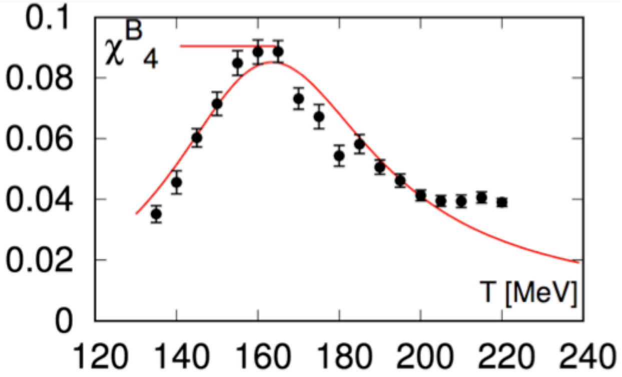

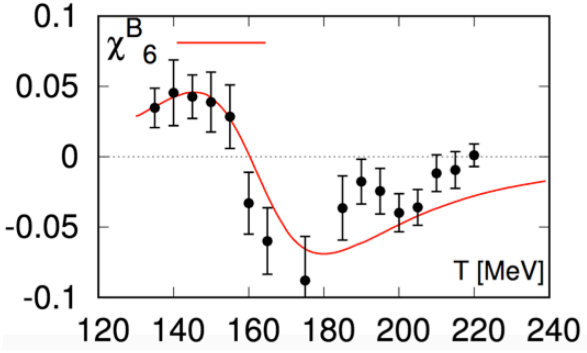

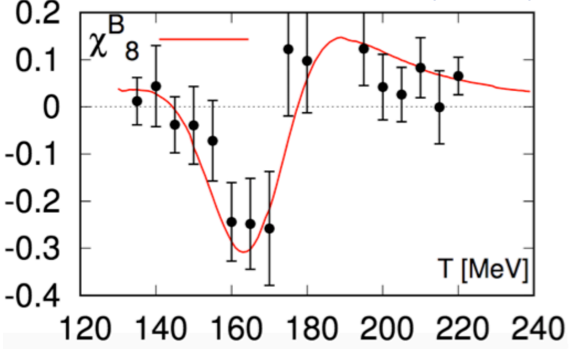

Freeze-out parameters from B fluctuations

- Thermometer: $\frac{\chi_3^B(T,\mu_B)}{\chi_1^B(T,\mu_B)}$ $=S_B\sigma_B^3/M_B$ Baryometer: $\frac{\chi_1^B(T,\mu_B)}{\chi_2^B(T,\mu_B)}$ $=\sigma_B^2/M_B$

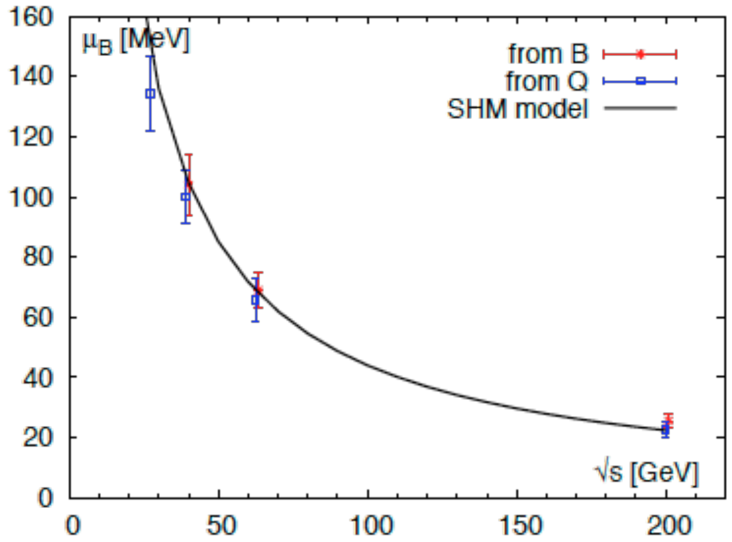

$\sqrt{s}[GeV]$	μ_B^f [MeV] (from B)	μ_B^f [MeV] (from Q)
200	25.8±2.7	22.8±2.6
62.4	69.7±6.4	66.6±7.9
39	105±11	101±10
27	-	136±13.8

WB: S. Borsanyi et al., PRL (2014)
STAR collaboration, PRL (2014)

Upper limit: $T_f \leq 151\pm4$ MeV

Consistency between freeze-out chemical potential from electric charge and baryon number is found.

A few Lessons learned

- Heavy ion collisions:
  - Phase transition at small μ_B is a smooth crossover
  - If a critical point exists, it is in the 3D-Ising model universality class
  - Equation of state and phase diagram are known from 1^{st} principles at $\mu_B/T<3.5$
  - Quark-Gluon Plasma is a strongly coupled fluid with very small viscosity/entropy
- Neutron star mergers:
  - GWs travel essentially at the speed of light
  - binary neutron star mergers are progenitors of short gamma ray bursts
  - they are prolific sites for the formation of heavy elements
  - constrained neutron-star radii to be between 9.5 and 13 km

Anatomy of a heavy-ion collision